Structural, electronic and magnetic properties of some early vs late transition dimetallaborane clusters - A theoretical investigation

Kandasamy Bharathi, Lalshab Beerma, Chinnasamy Santhi, Bellie Sundaram Krishnamoorthy, Jean-François Halet

For the table of contents use only

Structural, electronic and magnetic properties of some early vs late transition dimetallaborane clusters - A theoretical investigation

Kandasamy Bharathi[a], Lalshab Beerma[a], Chinnasamy Santhi[a], Bellie Sundaram Krishnamoorthy[a,b,*] and Jean-François Halet[b,*]

[a]*Department of Chemistry, Vivekanandha College of Arts and Sciences for Women (Autonomous), Elayampalayam, Tiruchengode, 600 036, India*

[b]*Institut des Sciences Chimiques de Rennes, UMR 6226 CNRS-Université de Rennes 1, Avenue du Général Leclerc, 35042 Rennes Cédex, France*

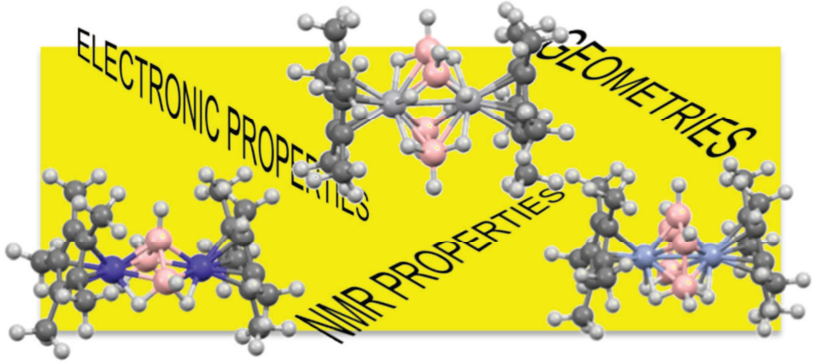

Structural, electronic and magnetic properties of some early vs late transition dimetallaborane clusters - A theoretical investigation

Kandasamy Bharathi[a], Lalshab Beerma[a], Chinnasamy Santhi[a], Bellie Sundaram Krishnamoorthy[a,b,*] and Jean-François Halet[b,*]

[a]*Department of Chemistry, Vivekanandha College of Arts and Sciences for Women (Autonomous), Elayampalayam, Tiruchengode, 600 036, India*

[b]*Institut des Sciences Chimiques de Rennes, UMR 6226 CNRS-Université de Rennes 1, Avenue du Général Leclerc, 35042 Rennes Cédex, France*

ABSTRACT. The strength of DFT methods in analyzing the electronic and magnetic properties of a series of dimetallaboranes of varied stoichiometry and architectural core, namely M_2B_3, M_2B_4 and M_2B_5 with both early- and late-transition metals is demonstrated. In particular, the observed ^1H and ^{11}B chemical shifts of most of the studied compounds are reproduced with a good accuracy of a few ppm at the DFT-GIAO BP86/TZ2P/SC level for the compounds with first-row transition metal elements and at the B3LYP/TZ2P/SO level for those with second- and third-row transition metal elements. This allows structural applications in elucidating the number and the location of bridging hydrogen atoms in experimentally poorly characterized metallaboranes such as $(Cp^*Cr)_2B_4H_8$.

Dedicated to Prof. Michael Mingos on the occasion of his 70th birthday in recognition of his major contributions to cluster chemistry.

Keywords: Cluster compounds . Density functional theory . Metallaborane complexes. NMR spectroscopy

* Corresponding authors. *E-mail addresses:* bskimo@yahoo.co.in (B. S. Krishnamoorthy) and halet@univ-rennes1.fr (J. -F. Halet)

Introduction

Although the proven methods for the formation of compounds containing metal-boron bonds are rather limited, there are today a plethora of metallaborane compounds, which have been synthesized and characterized with nearly all the transition metals, early and late metals [1]. Among them, dimetallaboranes constitute a larger part, with almost one hundred of them known and structurally and/or spectroscopically characterized [2-22]. Although the chemistry of these dimetallaboranes is experimentally growing rapidly, theoretical studies on these species are still rather scarce, despite the need to investigate and rationalize viz., (i) their structural diversity, (ii) their thermal and kinetic stability, (iii) their isomeric preferences, (iv) their chemical bonding, (v) their spectroscopic properties, etc. In particular, quantum chemical computations of ^{11}B and ^{1}H NMR chemical shifts have become one of the principal means of characterization of metallaborane compounds. These computations can even sometimes "rival that of X-ray crystallography" [24]. Density-functional theory (DFT) computations for instance can nowadays provide usefully precise chemical shifts as a function of the geometrical structure [25]. This has been shown by the past for some metallacarboranes for instance [26,27]. Recently, we have used such methods to tackle with some success the structural, electronic, and NMR properties of specific examples of dimetallaboranes [29-32].

For the latter, accuracies of about 2 to 3 ppm were achieved for the computed ^{11}B chemical shifts at the B3LYP/TZ2P all-electron relativistic scalar ZORA level of theory. Indeed, we have shown that although they are very computationally demanding, ^{11}B NMR chemical shift calculations at this level of theory using BP86/TZ2P/SC optimized geometries improves

considerably (by ca. 5-10 ppm) the computed values with respect to those obtained at the GGA/TZ2P all-electron relativistic scalar ZORA level, for early *4d* transition metal-borane systems (dimolybdaboranes, ditantalaboranes) [29,30]. On the other hand, only 1-2 ppm of improvement is observed for the metallaboranes with late *4d* transition metal (diruthenaboranes for instance) [31]. This drove us to look at the suitability of DFT methods using different GGA vs. hybrid functionals to accurately compute ^{11}B NMR chemical shifts in metallaboranes in general. For this purpose a series of dimetallaboranes of varied stoichiometry and architectural cores, namely M_2B_3, M_2B_4 and M_2B_5, with early and late transition metals has been chosen and studied (Chart 1). It would have been desirable to compare results on early- and late-transition-metal boranes with the same architecture, but it has been shown experimentally that early transition metals often lead to the formation of rather highly condensed metallaborane clusters (of M_2B_4 and M_2B_5 core), such as compounds **1-9** (Chart 1) discussed in this work, for example [13,33,34] whereas late-transition elements usually form stable metallaboranes with more open structures (with M_2B_3 core), such as compounds **15-17** (Chart 1) discussed in this work, for example [35]. Here we report that the observed ^{11}B NMR chemical shifts are reproduced with a reasonable accuracy at the BP86/TZ2P/SC level for the *3d* metallaboranes. On the other hand, the B3LYP/TZ2P/SO level (SO = spin-orbit) is necessary for *4d* and *5d* metallaboranes using BP86-optimized molecular geometries. This suggests that this particular combination of DFT levels is suitable for metallaboranes in general.

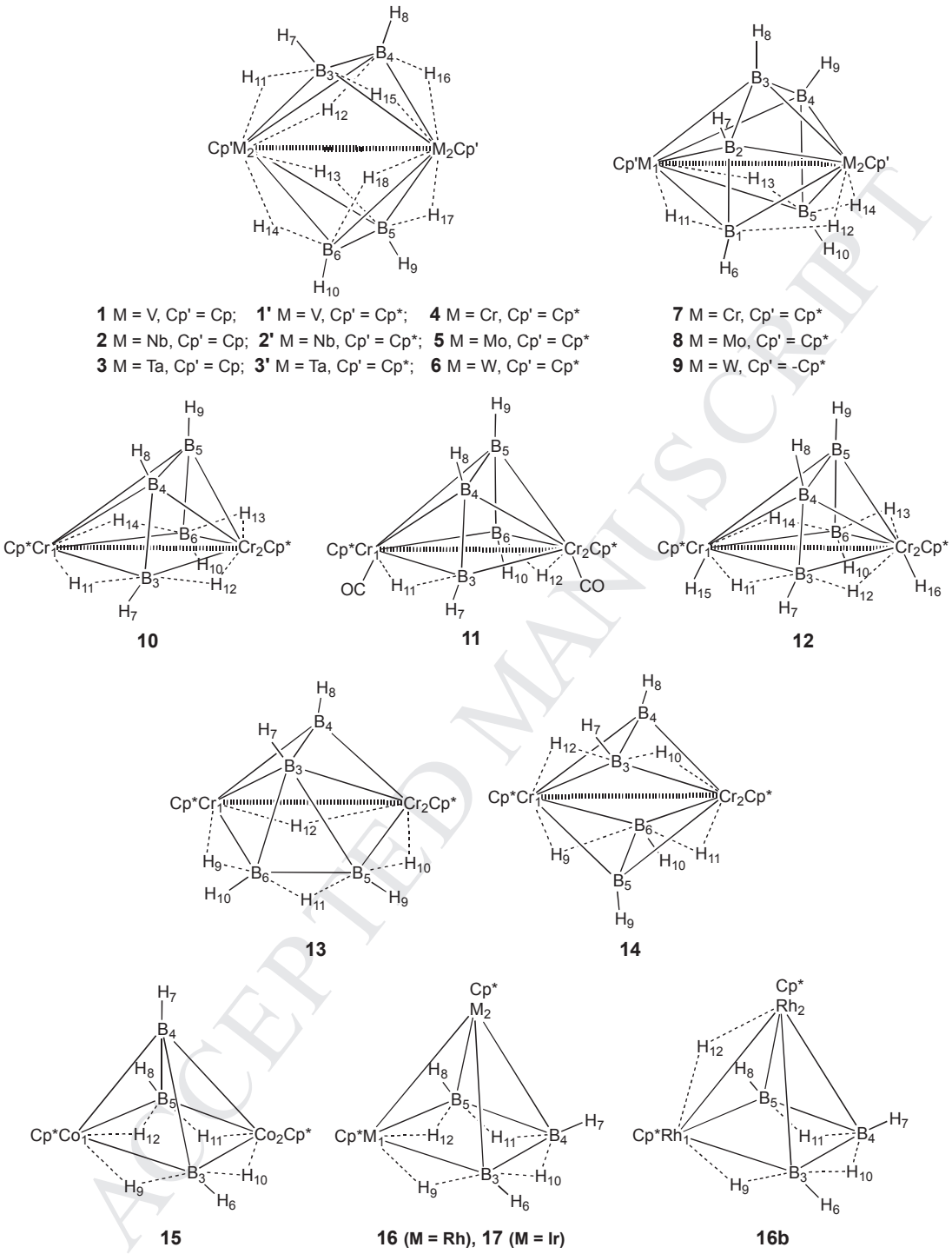

Chart 1. Examples of M_2B_3, M_2B_4 and M_2B_5 dimetallaborane cluster compounds.

Computational details

Density functional theory calculations were carried out using the Amsterdam Density Functional (ADF) program [36] developed by Baerends and co-workers [37]. The Vosko-Wilk-Nusair parameterization [38] was used for the local density approximation (LDA) with gradient corrections for exchange (Becke88) [39,40] and correlation (Perdew86) [41]. The geometry optimization procedure was based on the method developed by Versluis and Ziegler [42]. Relativistic corrections were added using the ZORA (zeroth order regular approximation) scalar Hamiltonian [43-45]. Structures were optimized using an all-electron TZ2P basis sets [36], available in the ADF program without any geometrical constraint. Experimental geometries were taken as inputs for compounds when they were available. The nature of the stationary points after optimization was checked by calculations of the harmonic vibrational frequencies to ensure that genuine minima were obtained.

The BP86/TZ2P optimized geometries were then used as inputs for the NMR computations using all-electron TZ2P basis sets [36,38] at the relativistic scalar (SC) ZORA level of theory. NMR chemical shifts were also calculated with the hybrid Becke-Lee-Yang-Parr (B3LYP) functional [46-48] for comparison, using the BP86/TZ2P optimized geometries. The computation of the NMR shielding tensors employed gauge-including atomic orbitals (GIAOs) [49-52], using the implementation of Schreckenbach, Wolff, Ziegler, and co-workers [53-57]. NMR calculations were performed including the spin-orbit (SO) term with both BP86 and B3LYP functionals. TMS ($SiMe_4$) was used as an internal standard for the ^{1}H NMR. The projected ^{11}B chemical shielding values, determined from relativistic scalar ZORA calculations were referenced to B_2H_6 as the primary reference point, and these chemical shift values (δ) were then converted to the standard BF_3•OEt_2 scale using the experimental value of +16.6 ppm for B_2H_6.

Results and discussion

Geometries

Precise structural arrangements are necessary for getting accurate ^{11}B and ^{1}H NMR chemical shifts [58]. Different M_2B_3, M_2B_4 and M_2B_5 clusters were then geometrically optimized and compared to experimental data where available. We commence with the $(Cp'M)_2(B_2H_6)_2$ cluster compounds (Cp' = C_5H_5 (Cp) or C_5Me_5 (Cp*); M = V, Nb, Ta). Salient optimized geometrical parameters are collected in Table 1. The three representatives with Group 5 metals were characterized crystallographically and spectroscopically with either Cp in the cases of $(CpV)_2(B_2H_6)_2$ (**1**) [59] and $(CpNb)_2(B_2H_6)_2$ (**2**) [59] or Cp* in the case of $(Cp^*Ta)_2(B_2H_6)_2$ (**3'**) [59]. Overall, the optimized bond lengths reproduce the X-ray data rather well, within a few hundredths of Å, a degree of agreement which is typical for the DFT level employed. The computed M-M bond distances of 2.735 Å, 2.954 Å, and 2.941 Å are comparable to the corresponding X-ray values of 2.787(2) Å, 2.948(16) Å, and 2.933(4) Å, respectively, for clusters **1**, **2** and **3'**. The average M-B bond lengths in these compounds of 2.269 Å, 2.405 Å, and 2.387 Å are substantially longer than the sum of the M and B covalent radii, i.e., 2.20 Å, 2.22 Å, and 2.22 Å for V-B, Nb-B, and Ta-B, respectively [60], supporting the presence of hydrogen atoms bridging M-B bonds. Comparing the computed and experimental B-B bond lengths indicates that the computed ones are 0.02 Å longer for **1** and **3'**, but 0.04 Å shorter for **2**. Finally, we note that geometries computed either with Cp or Cp* as ancillary ligands attached to the metal atoms are highly similar.

For the Group-6 metal triad, only the molecular structures of $(Cp^*Mo)_2(B_2H_6)_2$ (**5**) and $(Cp^*W)_2(B_2H_6)_2$ (**6**) were proposed with an arrangement similar to that encountered for the

Group-5 metal triad discussed above, on the basis of the ^{11}B, ^{1}H NMR and mass spectrometry details [19,20]. They were computed as well as the hypothetical Cr homolog $(Cp^*Cr)_2(B_2H_6)_2$ (**4**). BP86/TZ2P optimized geometries show M-M bond lengths of 2.760 Å, 2.900 Å, and 2.909 Å for compounds **4**, **5**, and **6**, respectively (Table 1). The latter for instance is notably longer than the W-W bond length of 2.8174(8) Å reported for $(Cp^*W)_2B_5H_9$ for instance [19,20], but still short enough to indicate some significant metal-metal bonding interactions at first sight. The rather long computed average M-B bond lengths (2.4015 Å for W-B for instance compared to 2.239 Å in $(Cp^*W)_2B_5H_9$, vide infra) may be due to the presence of eight bridging hydrogen atoms. The B-B bond lengths in compounds **4**, **5** and **6** are considerably shorter (1.671 Å, 1.690 Å, 1.686 Å) than normal B-B single bonds observed for the related compounds **1**-**3** (ca.1.75 Å), reflecting strong B-B bonding interactions in these clusters.

For the *oblato-nido* clusters $(Cp^*M)_2B_5H_9$ (M = Cr (**7**), Mo (**8**), W (**9**)), the core of which depicts a hexagonal bipyramid with one missing equatorial vertex, the BP86/TZ2P/SC optimized geometries are in good agreement with the metrical parameters measured experimentally by X-ray crystallography (see Table ST1, Supporting Information). The computed M-M bond distances of 2.592 Å, 2.810 Å and 2.835 Å nicely reproduce the experimental ones which are 2.625(9) Å [15], 2.8085(6) Å [30], and 2.817(8)Å [19,20] for **7**, **8**, and **9**, respectively. They indicate significant metal-metal bonding interactions in these clusters.

As said above, the Cr compound $(Cp^*Cr)_2(B_2H_6)_2$ (**4**) has not been reported so far. With a Cr_2B_4 core, the compound $(Cp^*Cr)_2B_4H_8$ (**10**) has been characterized instead with a *nido* pentagonal bipyramidal cage with one missing equatorial vertex and the two Cr atoms occupying the axial positions and separated by 2.870(2) Å (Chart 1) [61]. The reaction of **10** with CO yielded $(Cp^*Cr)_2B_4H_6(CO)_2$ (**11**, Chart 1) as the major product [14]. The same *nido* pentagonal

bipyramidal Cr_2B_4 cage was confirmed by an X-ray analysis with a Cr-Cr bond length 2.792(1) Å [14]. A DFT geometry optimization of **10** at the BP86/TZ2P/SC all-electron scalar ZORA level resulted in a structure with a Cr1-Cr2 bond length abnormally short of 2.548 Å (Table 2), suggesting that the chemical formula of **10** reported experimentally might be wrong (hydrogen atoms were not directly located from the X-ray analysis [14]). Due to the large difference with the experimental value (0.322 Å), two hydrogen atoms bridging the Cr1-B4 and Cr2-B5 vectors were added (see **10** in Chart 1). The optimized structure resulted in the B3-B4 bond breakage. The two hydrogen atoms were then terminally added to two Cr atoms analogously to the CO ligand in **11**. Interestingly, the optimized geometry of this model structure $(Cp^*Cr)_2B_4H_{10}$ (see **12** in Chart 1) revealed a Cr_2B_4 open cage similar to that computed for **10** but with a Cr1-Cr2 bond length considerably longer of 2.7356 Å, still 0.13 Å shorter than the experimental value experimentally measured for $(Cp^*Cr)_2B_4H_8$ (**10**) but relatively close to the Cr-Cr bond length experimentally observed in $(Cp^*Cr)_2B_4H_6(CO)_2$ (**11**), 2.792(1) Å which compares rather well to the computed distance of 2.764 Å (Table 2). The comparison of the computed B-B distances in **10** and **12** with those reported experimentally, are not much informative about the 'right' formula. The B3-B4, B4-B5, B5-B6 distances of **10** are 1.735, 1.637, 1.725 Å, respectively, whereas those in the model compound $(Cp^*Cr)_2B_4H_{10}$ **12**, are 1.701, 1.639, 1.702 Å, respectively. They all deviate somewhat from the corresponding experimental (not very precise) X-ray values which are 1.75(3), 1.75(3), 1.61(3) Å, respectively. Notably, the Cp* ligands are not parallel but tilted away from the open face of the cluster cage with angles of 28.1(8)° and 30.4(20)° experimentally measured for **10** and **11**, respectively [14,61,63]. Interestingly, the Cp* rings are hardly tilted in the optimized geometry of **10** but significantly tilted in **11** and **12** (16° and 14°, respectively). Additional structural arrangements can be envisaged for this compound,

such as a capped square pyramidal (**13**) or $(Cp^*Cr)_2(B_2H_4)_2$ (**14**) structures with symmetrical (B_2H_4) units (Chart 1) [61]. Their geometry optimization results in Cr-Cr bond lengths of 2.22 and 2.42 Å, respectively. That in the former is comparable to the Cr-Cr triple bond of 2.200(3) encountered in $Cp_2Cr_2(CO)_4$ [64] for instance.

The late-transition metal borane compounds of formula $(Cp^*M)_2B_3H_7$ have been crystallographically characterized for M = Co (**15**) [5] and Rh (**16**) [7] (Chart 1). They display a square pyramidal geometrical cage with two metal atoms occupying basal positions in the case of **15** (*nido*-2,4-$(Cp^*Co)_2B_3H_7$) and one metal atom occupying the apical position and the second metal atom occupying one basal position in the case of **16** (*nido*-1,2-$(Cp^*Rh)_2B_3H_7$). Interestingly, there is an M-M bond in the latter but not in the former. A tautomer of **16**, i.e., *nido*-1,2-$(Cp^*Rh)_2(\mu\text{-H})B_3H_6$ (**16b**) was also spectroscopically observed [7]. The optimized distances are in a rather good agreement with the experimentally available X-ray values (Table 2, Table ST3, Supporting Information). The computed Rh-Rh bond length in **16** is 2.740 Å, 0.05 Å larger than the X-ray value of 2.6892(3) Å [7]. This deviation might be attributed to the presence of two independent molecules in the unit cell, with a disordered Cp* ring in one molecule, and the fully disordered second molecule, observed in the solid state X-ray structure [7]. This distance is notably shorter than the Rh-Rh bond length of 2.8478(11) Å reported for the *nido*-2,4-$(Cp^*Rh)_2B_3H_6$ Cl cluster for which the two rhodium atoms occupy two adjacent basal positions [7]. Geometry optimization of **16b** results in an intermediate Rh-Rh bond length of 2.744 Å. A very small energy difference, 0.26 kcal/mol, is computed between tautomers **16** and **16b** in favor of the former. The iridium analogue $(Cp^*Ir)_2B_3H_7$ (**17**) has not been isolated until now. BP86/TZ2P metrical parameters computed with the same arrangement as its Rh congener **16** are comparable to those measured in related diiridium cluster compounds [8]. For example,

the computed Ir-Ir bond length of 2.7733 Å is somewhat shorter than that in *arachno*-$(Cp^*IrH)_2(\mu\text{-}H)B_2H_5$ which is 2.8227(8) Å [8] but similar to the value of 2.7814(9) Å measured in *arachno*-$(Cp^*IrH)_2B_4H_8$ [8].

Electron counts and electronic structures

Dimetallaboranes of the earlier transition metals often present interesting challenges to the well-established cluster electron-counting rules, the so-called Polyhedral Skeletal Electron Pair Theory (PSEPT) [65,70], due to their distinctly oblate (flattened along the M‑M cross-cluster axis) rather than closely spherical nature [1,13,71,72]. They are generally characterized with short metal-metal cross-cluster distances and *apparent* formal cluster electron counts a few skeletal electron pairs (sep) less (generally three) than required for canonical *closo*- or *nido*-structure of the same nuclearity. Previous DFT calculations suggested that these *oblato* arrangements are indeed very stable compounds, due to an intricate mutual interaction of the dimetal fragment and the borane cage. Indeed, some of us showed that bringing two CpM or Cp*M fragments close together generates a set of three frontier metal orbitals that can only interact with the frontier orbitals of the borane fragment. These orbitals on each of these complementary fragments, which normally would be filled in a late transition-metal metallaborane with a spherical deltahedral shape, interact strongly to generate three low-lying filled orbitals and three high-lying unfilled orbitals. As a result, they generate a metal-metal cross-cluster bonding where the *effective* sep counts (p + 1 (*oblato-closo*), p + 2 (*oblato-nido*), p + 3 (*oblato-arachno*) if p is the number of occupied vertices) is three seps larger than the *apparent* sep count obtained via the classical PSEPT [1,13,73].

If these PSEPT-extended rules are applied to compounds **1-3** and **1'-3'**, they can be viewed as *oblato-arachno* species with a structure derived from an 8-vertex *oblato-closo* hexagonal bipyramidal cluster encountered for the effective 9-sep cluster $(Cp^*Re)_2B_6H_4Cl_2$ [13], with two non-adjacent vacant sites. Indeed, they have the same effective sep count of 9 ([-2 (Cp'M) x 2 + 2 (BH) x 4 + 1 (bridging H) x 8 + 6 (t_{2g} M_2)] / 2), in agreement with a somewhat short metal-metal cross-cluster bond. Surprisingly enough, clusters **4-6** with the same *oblato-arachno* hexagonal bipyramidal core possess an effective sep count of 10 ([-1 (Cp*M) x 2 + 2 (BH) x 4 + 1 (bridging H) x 8 + 6 (t_{2g} M_2)] / 2), i.e., one more that the expected electron count. In the same manner, clusters **7-9** can be viewed as *oblato-nido* M_2B_5 species also derived from an 8-vertex *closo* hexagonal bipyramidal cluster, possessing the expected effective sep count of 9 ([-1 (Cp^*M) x 2 + 2 (BH) x 5 + 1 (bridging H) x 4 + 6 (t_{2g} M_2)] / 2].

With only 8 hydrogen atoms cluster $(Cp^*Cr)_2B_4H_8$, **10** possesses 8 sep's [-1 (Cp^*Cr) x 2 + 2 (BH) x 4 + 1 (bridging H) x 4 + 6 (t_{2g} M_2)] / 2), the expected count if it is assumed that the Cr_2B_4 core depicts an open *nido* pentagonal bipyramidal cage. This implies that the carbonyl analog **11** which adopts the same polyhedral cage, has 9 sep's, i.e., one more than expected. A close examination of the X-ray structures of **10** and **11** and the optimized geometries of **10-12** (B3-B4-B5 bond angles and non-bonded B3-B6 distance) indicates that in turn, **10** and **11** are better considered as *oblato-arachno* hexagonal bipyramidal clusters, deriving from an 8-vertex *closo* hexagonal bipyramid by removal of two adjacent basal vertices. Consequently, **10** is an electron-deficient species, whereas **11** (and **12** which possesses 10 hydrogen atoms) possess the expected count of sep's. Fehlner et al. already noted the electronic unsaturation of **10** on the basis of its reactivity and a molecular orbital analysis using semi-empirical Fenske-Hall calculations [63]. The model clusters **13** and **14** [61,62] also result in an effective sep count of five. The shortage of

skeletal electrons in cluster **14** is compensated by a formal Cr-Cr triple bond and thus, in some ways, related to the two-electron richer $(CpNbCO)_2(RCCR)_2$ compound (M=M double bond) as theoretically pointed out by Hoffmann and colls. [74].

Satisfactorily, all late-transition metal compounds **15-17** with a *nido* square pyramidal M_2B_3 cage and a 7-sep count ([2 (Cp*M) x 2 + 2 (BH) x 3 + 1 (bridging H) x 4] / 2) obey the classical PSEPT rules, as expected.

When dealing with electron counting, it is of major importance not to forget that all the rules, which govern the structure/electron count relationship, are based on the so-called the 'closed-shell principle' [1,73]. In other words, these stable dimetallaboranes should exhibit a significant highest occupied molecular orbital (HOMO)–lowest unoccupied molecular orbital (LUMO) energy gap. Indeed, BP86/TZ2P/SC HOMO-LUMO gaps of ca. 2 eV are computed for many of the studied compounds in agreement with their electron counts (Table ST4, Supporting Information). $(Cp^*Cr)_2(B_2H_6)_2$ (**4**) has not been isolated yet and its heavier congeners **5** and **6** have only been characterized in solution [19,20]. They are too much electron-rich by one extra sep according to the PSEPT-extended rules (see above). Accordingly, a small HOMO-LUMO gap of only 0.71eV was computed for the non-reported species **4**. Larger energy gaps of 1.42 and 1.51 eV were computed for **5** and **6**, respectively. For the 'unsaturated' cluster **10**, a small HOMO-LUMO gap of only 0.65 eV, which does not militate for its existence, led us to look into the details of the structure. A HOMO-LUMO gap of 1.64 eV is computed for **11** which has two electrons more. With two hydrogen atoms more, the HOMO-LUMO gap jumps to 2.21eV for model **12**, isoelectronic to **11**. Additionally, HOMO-LUMO gaps of 1.57 and 0.98 eV are computed for the model compounds **13** and **14**, respectively. Obviously, these results render the formula of **10** questionable.

NMR chemical shifts

The number of direct metal−boron and boron−boron bonds, the presence or absence of bridging hydrogen atoms, the metal identity, the atomic coordination number, the atom charges are some parameters which may influence ^{1}H and ^{11}B NMR chemical shifts in metallaboranes [58]. ^{11}B, ^{1}H and ^{13}C NMR chemical shifts were calculated at the DFT level using both BP86 and hybrid B3LYP functionals, with and without scalar spin-orbit (SO) relativistic corrections, using BP86 optimized geometries. Data are collected in Tables 3-5 and Tables ST5 and ST6 (Supporting Information) together with the experimental values where available. It turns out overall that the B3LYP/TZ2P/SO ZORA calculated isotropic magnetic shielding constants (converted to ^{11}B, ^{13}C and ^{1}H NMR chemical shifts) agree very well with experimental data for clusters with the second and third row early-transition metals Nb, Ta, Mo and W, whereas BP86/TZ2P/SC computed values are in a better agreement for the clusters containing the first row early-transition metals V and Cr. The importance of both scalar and spin-orbit relativistic corrections for the shielding tensors in heavy transition metal complexes was observed previously by Autschbach et al. [75]. Bridging hydrogen atoms in these clusters are relatively shielded and resonate around -6 to -12 ppm.

A single ^{11}B NMR resonance is experimentally observed at 1.7 ppm for $(CpV)_2(B_2H_6)_2$ (**1**) and $(CpNb)_2(B_2H_6)_2$ (**2**) and at -4.0 ppm for $(Cp^*Ta)_2(B_2H_6)_2$ (**3'**), revealing the symmetrical nature of these structures in solution [59]. DFT calculations also predict the symmetrical nature of these clusters. In the case of **1**, the ^{11}B NMR chemical shifts computed at the BP86/TZ2P and B3LYP/TZ2P levels deviate downfield from the experimental values only by 4 ppm for the former but 17.5 ppm for the latter (Table 3). For the carbon atoms of the Cp ligands, a reverse

situation, but less pronounced is computed with a maximum deviation of 6 ppm upfield at the BP86/TZ2P/SC level and only 1 ppm at the B3LYP/TZ2P/SC level when compared to the experimental ^{13}C NMR chemical shifts. On the other hand, both BP86/TZ2P/SC and B3LYP/TZ2P/SC computed ^{1}H NMR chemical shift values are in good agreement with the experimental ones with a maximum deviation of 1 ppm. For **2**, the more accurate^{11}B NMR chemical shifts are computed at the B3LYP/TZ2P/SO level (only slightly better than without SO inclusion) with a maximum deviation of only 0.5 ppm downfield whereas the BP86/TZ2P/SO computed values deviate by 2 ppm upfield. For the ^{13}C NMR, the maximum deviation obtained at the B3LYP/TZ2P/SO and BP86/TZ2P/SO levels are 6 ppm and 2.5 ppm downfield, respectively. Both B3LYP and BP86 methods are successful in predicting the ^{1}H NMR values with a maximum deviation of 1.5 ppm. In the case of the tantalum cluster **3'**, ^{11}B NMR chemical shifts computed at the B3LYP/TZ2P level including SO contributions result in a good agreement with the experimentally observed values with a maximum deviation of 3 ppm upfield (7 ppm at the BP86/TZ2P/SO level). We note that the inclusion of the SO term increases considerably the accuracy. The ^{13}C NMR chemical shift values are computed with a maximum deviation of 3 ppm at the BP86/TZ2P/SC level and 6 ppm at the B3LYP/TZ2P/SC level. Though the inclusion of SO term has a considerable effect on ^{11}B NMR chemical shifts, only a small effect (0.3 ppm) is observed for the chemical shifts of the methyl and cyclopentadienyl carbon atoms. The computed ^{1}H NMR chemical shifts for the terminal and bridging hydrogen atoms are comparable at both B3LYP/TZ2P/SO and BP86/TZ2P/SO levels with deviations of 1-2 ppm.

When comparing compounds **1**, **2**, and **3'**, i.e., from V to Ta, the boron atoms and the bridging hydrogen atoms experience slightly more shielding but the reverse situation is observed for terminal hydrogen atoms. A look at the individual B3LYP/TZ2P/SO computed components

$\sigma_{(dia)}$, $\sigma_{(para)}$, and $\sigma_{(so)}$ of the shielding tensors indicates that the diamagnetic shielding largely dominates in all the cases as expected and is comparable in all clusters (Fig. 1). On the other hand, the paramagnetic shielding decreases considerably while going from V to Ta, from -105 ppm to -71 ppm. Not surprisingly, the shielding from the relativistic spin-orbit term strongly increases from -0.3 for V and Nb to -7.0 ppm for Ta. In fact, the large low-field shifts, which are characteristics of the effect of the neighboring transition metals on ^{11}B NMR resonances, were already ascribed to the paramagnetic term by Fehlner et al. [34].

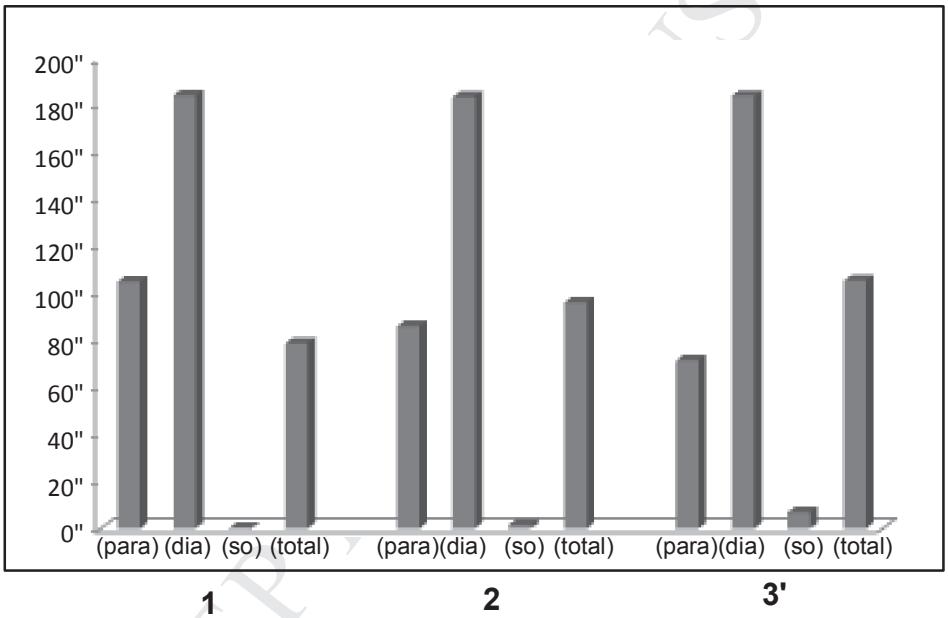

Fig. 1. Individual components of shielding tensors (ppm) $\sigma_{(para)}$, $\sigma_{(dia)}$ and $\sigma_{(so)}$ vs. total shielding in ^{11}B NMR of compounds **1**, **2**, and **3'**. $\sigma_{(para)}$ and $\sigma_{(so)}$ are plotted as $|\sigma_{(para)}|$ and $|\sigma_{(so)}|$.

For the metallaborane clusters $(Cp^*Mo)_2(B_2H_6)_2$ (**5**) and $(Cp^*W)_2(B_2H_6)_2$ (**6**), a single signal in the ^{11}B NMR is also experimentally observed supporting the highly symmetric nature of these clusters in solution. For **5** a signal is observed experimentally at -58.6 ppm in the low frequency region. With the BP86 functional, deviations up to 6 ppm (without SO) or 7 ppm (with SO) in

the upfield region are calculated (Table 4). Maximum deviations of upfield 2 ppm (without SO) and 4 ppm (with SO) are computed with the B3LYP functional. More surprisingly, the ^{11}B NMR signal computed for **6** compares moderately to that experimentally measured at -53.9 ppm. The closest computed value, which deviates by 10 ppm, is obtained at the B3LYP level (without SO). A good agreement between theory and experiment (0-2 ppm deviation) is observed for the ^{1}H NMR chemical shifts of the terminal and bridging hydrogen atoms with both methods (without SO).

NMR data measured experimentally suggest that the electron-deficient cluster $(Cp^*Cr)_2B_4H_8$, **10**, is diamagnetic [61]. Two distinct boron environments are expected from a doublet signal at 126.5 ppm and a multiplet signal at 34.3 ppm (Table 5). Interestingly, the BP86/TZ2P computed values of 15.9, 22.4, 22.2, and 16.6 ppm for B3, B4, B5, and B6, respectively, strongly differ, especially those for B4 and B5. With two hydrogen atoms more, the corresponding values change to 36.6, 32.4, 33.6, and 37.2 ppm. A good agreement with the experimental values is then observed for B3 and B6, but again not for the experimentally unusually shielded B4 and B5 atoms. These results suggest that compound **10** should probably be corrected into $(Cp^*Cr)_2B_4H_{10}$, **12**, and that the experimental boron chemical shifts of 126.5 ppm have been wrongly attributed to B4 and B5 atoms. Concerning, the ^{1}H NMR chemical shifts, the best agreement is observed between values experimentally measured for **10** and values theoretically computed for **12**. For comparison, the ^{11}B NMR chemical shifts were computed for the cluster $(Cp^*Cr)_2B_4H_6(CO)_2$ (**11**) for which the two corresponding signals are experimentally observed at 63.9 and 34.9 ppm. A good agreement is found at either at BP86 or B3LYP levels of theory (Table 5).

^{11}B NMR chemical shifts of the two types of boron atoms (B2, B3 and B4) directly bonded to the metal atoms in $(Cp^*M)_2B_5H_9$ (M = Cr (**7**), Mo (**8**), W (**9**)) experience a large systematic shift to higher field going from Cr to Mo to W, whereas the shift at upper field for the boron atoms (B1, B5) connected to the metal atoms via M-H-B bridged bonds are invariant (Table ST5 (Supporting Information) and Fig. 2). This trend is also predicted by the DFT calculations, although the agreement between computed and experimental values is far to be satisfactory. For **7** the better chemical shifts are computed at the BP86/TZ2P/SC level with a deviation of 3.5 ppm for B1/B5, but 13 ppm for B2/B4 and 18 ppm for B3 downfield. Except for B3 for which a deviation of 9 ppm is observed, the computed B3LYP/TZ2P/SC values differ by more than 20 ppm downfield. On the other hand, B3LYP/TZ2P/SC computed values for the Mo analogue **8** and B3LYP/TZ2P/SO computed values for the W analogue **9** are in a very good agreement with the experimental values with a maximum deviation of 3 ppm downfield (Table 4 and Fig. 2). Inclusion of relativistic spin-orbit corrections for the latter improves the B3LYP/TZ2P/SC computed ^{11}B NMR chemical shifts considerably by ca. 7 ppm. Both B3LYP and BP86 computed ^{1}H NMR δ values for the B-H terminal and M-H-B bridging hydrogen atoms in close agreement with the experimental values with a maximum deviation of ca. 1 ppm.

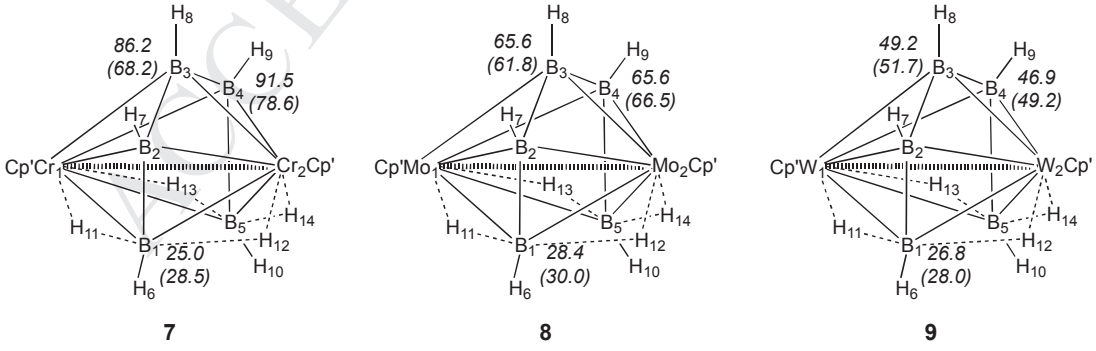

Fig. 2. Experimental and most accurate computed (in brackets) ^{11}B NMR chemical shifts (ppm) for compounds **7**-**9** (BP86/TZ2P/SC for **7**, B3LYP/TZ2P/SC for **8**, and B3LYP/TZ2P/SO for **9**).

^{11}B NMR chemical shifts were also computed for the late transition metal borane compounds in order to also check the suitability of the computational method used (Table ST6 and Fig. 3). Experimentally, the *nido*-2,4-$(Cp^*Co)_2B_3H_7$ compound **15** exhibits two ^{11}B NMR signals in a 2:1 ratio at 65.8 ppm and -18.1 ppm [5]. Correct values (Table 10) with deviations of a few ppm are computed at the BP86/TZ2P/SC, BP86/TZ2P/SO, and B3LYP/TZ2P/SC levels (the latter is slightly better). Good values are also computed for the ^{1}H NMR chemical shifts, especially at the B3LYP/TZ2P/SC level with maximum deviations of ca. 1 ppm. The signals of the two terminal hydrogen atoms H6 and H8, not attributed experimentally are computed to resonate around 0 ppm, justifying the possibility of overlapping experimentally with the H peak of TMS [5] and the strength of the computational methods used. For the *nido*-1,2-$(Cp^*Rh)_2B_3H_7$ species **16**, the experimental ^{11}B NMR spectrum results with four broad signals at 3.1, 5.8, 8.2, and 11.1 ppm and a very broad signal at 21.1 ppm [7]. Since only three signals are expected, these five signals must be due to the presence of two tautomers (**16** and **16b** for instance, see above) or even other additional species in solution, as confirmed later with variable-temperature NMR [7]. Indeed, calculations seem to indicate a more complex situation. Although, the different levels of calculations lead to somewhat different values (up to 10 ppm difference), they show the same trend with the three boron atoms in **16** resonating in the same range around 0-10 ppm (Table 5 and Fig. 3), and the three boron atoms in **16b** resonating strongly differently around -12 (B3), 1 (B4) and 48 (B5) ppm. With no experimental peaks measured at such low or high frequencies, we might conclude that **16b** is not present in the solution of **16** and that the additional peak such as at 21 ppm are due to other species. Interestingly, the ^{11}B NMR peaks for the chlorine-analogue cluster $(Cp^*Rh)_2B_3H_6Cl$ show experimental ^{11}B NMR chemical shifts at 48.0, 4.0, and -5.3 ppm for the three boron atoms [11].

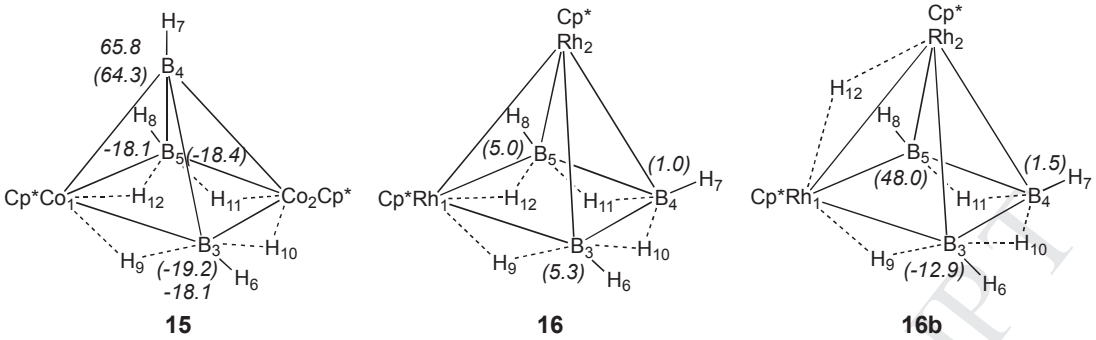

Fig. 3. DFT computed chemical shift values (ppm, in brackets) for clusters **15** (B3LYP/TZ2P/SC) and **16**, **16b** (B3LYP/TZ2P/SO). Experimental values for **15** are given for comparison.

Conclusion

The present study proves the strength of DFT methods in analyzing the electronic and magnetic properties of a series of dimetallaboranes with both early- and late-transition metals. In particular, the observed ^{1}H and ^{11}B chemical shifts of most of the studied compounds can be reproduced with a rather good accuracy of a few ppm at the DFT-GIAO BP86/TZ2P/SC level for the compounds with first-row transition metal elements and at the B3LYP/TZ2P/SO level for those with second- and third-row transition metal elements. This shows that the quality of DFT computed ^{1}H and ^{11}B chemical shifts generally attained for boranes and carboranes does not degrade much in the presence of transition metals, suggesting that any metallaborane is amenable to relatively accurate ^{1}H and ^{11}B NMR computations. Indeed, the accuracy is sufficient for structural applications to elucidate the number and the location of bridging hydrogen atoms in experimentally poorly characterized metallaboranes such as $(Cp^{*}Cr)_2B_4H_8$.

Acknowledgments

The authors acknowledge the Indo-French Centre for Promotion of Advanced Research (IFCPAR) (Project No. 4405-1) for generous financial support. Dr. B. Le Guennic (Rennes) is thanked for helpful discussions.

Appendix. Supplementary data

Supplementary data (Tables ST1-ST6 and Cartesian coordinates of all optimized geometries) related to this article can be found at http://dx.doi.org/10.1016/j.jorganchem…

References

[1] T. P. Fehlner, J.-F. Halet, J.-Y. Saillard, Molecular Clusters. A Bridge to Solid-State Chemistry, Cambridge University Press, New York, 2007.

[2] T. P. Fehlner, Organometallics 19 (2000) 2643-2651.

[3] R. B. King, Inorg. Chem. 43 (2004) 4241-4247.

[4] T. P. Fehlner, Organometallics 19 (2000) 2643-2651.

[5] Y. Nishihara, K. J. Deck, M. Shang, T. P. Fehlner, B. S. Haggerty, A. L. Rheingold, Organometallics 13 (1994) 4510-4522.

[6] X. Lei, M. Shang, T. P. Fehlner, J. Am. Chem. Soc. 120 (1998) 2686-2687.

[7] H. Yan, A. M. Beatty, T. P. Fehlner, Organometallics 21 (2002) 5029-5037.

[8] X. Lei, M. Shang, T. P. Fehlner, Chem. Eur. J. 6 (2000) 2653-2664.

[9] S. Ghosh, B. C. Noll, T. P. Fehlner, Dalton Trans. (2008) 371-378.

[10] K. Geetharani, S. K. Bose, G. Pramanik, T. K. Saha, V. Ramkumar, S. Ghosh, Eur. J. Inorg. Chem. (2009) 1483-1487.

[11] X. Lei, M. Shang, T. P. Fehlner, J. Am. Chem. Soc. 121 (1999) 1275-1287.

[12] A. S. Weller, M. Shang, T. P. Fehlner, Chem. Commun. (1998) 1787-1788.

[13] B. Le Guennic, H. Jiao, S. Kahlal, J.-Y. Saillard, J.-F. Halet, S. Ghosh, M. Shang, A. M. Beatty, A. L. Rheingold, T. P. Fehlner, J. Am. Chem. Soc. 126 (2004) 3203-3217.

[14] J. Ho, K. J. Deck, Y. Nishihara, M. Shang, T. P. Fehlner, J. Am. Chem. Soc. 117 (1995) 10292-10299.

[15] S. Aldridge, H. Hashimoto, K. Kawamura, M. Shang, T. P. Fehlner, Inorg. Chem. 37 (1998) 928-940.

[16] H. J. Bullick, P. D. Grebenik, M. L. H. Green, A. K. Hughes, J. B. Leach, P. C. McGowan, J. Chem. Soc. Dalton Trans. (1995) 67-75.

[17] S. Aldridge, M. Shang, T. P. Fehlner, J. Am. Chem. Soc. 120 (1998) 2586-2598.

[18] S. Sahoo, R. S. Dhayal, B. Varghese, S. Ghosh, Organometallics 28 (2009) 1586-1589.

[19] A. S. Weller, M. Shang, T. P. Fehlner, Organometallics 18 (1999) 53-64.

[20] S. K. Bose, S. Ghosh, B. C. Noll, J.-F. Halet, J.-Y. Saillard, A. Vega, Organometallics 26 (2007) 5377-5385.

[21] C. Ting, L. Messerle, J. Am. Chem. Soc. 111 (1989) 3449-3450.

[22] S. Aldridge, H. Hashimoto, M. Shang, T. P. Fehlner, J. Chem. Soc. Chem. Commun. (1998) 207-208.

[23] S. K. Bose, K. Geetharani, B. Varghese, S. M. Mobin, S. Ghosh, Chem. Eur. J. 14 (2008) 9058-9064.

[24] T. Onak, J. Tseng, M. Diaz, D. Tran, J. Arias, S. Herrera, D. Brown, Inorg. Chem. 32 (1993) 487-489.

[25] G. Schreckenbach, T. Ziegler, Theor. Chem. Acc. 99 (1998) 71-82.

[26] M. Bühl, D. Hnyk, J. Macháček, Chem. Eur. J. 11 (2005) 4109-4120.

[27] M. Bühl, J. Holub, D. Hnyk, J. Macháček, Organometallics 25 (2006) 2173-2181.

[28] M. Bühl, D. Hnyk, J. Macháček, Inorg. Chem. 46 (2007) 1771-1777.

[29] K. Geetharani, B. S. Krishnamoorthy, S. Kahlal, S. M. Mobin, J.-F. Halet, S. Ghosh, Inorg. Chem. 51 (2012) 10176 - 10184.

[30] B. S. Krishnamoorthy, A. Thakur, K. Chakrahari, S. Bose, P. Hamon, T. Roisnel, S. Kahlal, S. Ghosh, J.-F. Halet, Inorg. Chem. 51 (2012) 10375 - 10383.

[31] B. S. Krishnamoorthy, S. Kahlal, S. Ghosh, J.-F Halet, Theor. Chem. Acc. 132 (2013) 1356-1366.

[32] B. S. Krishnamoorthy, S. Kahlal, B. Le Guennic, J.-Y. Saillard, S. Ghosh, J.-F. Halet Sol. State Sci. 14 (2012) 1617–1623.

[33] S. K. Bose, S. M. Mobin, S. Ghosh, J. Organomet. Chem. 696 (2011) 3121-3126.

[34] A. S. Weller, T. P. Fehlner, Organometallics 18 (1999) 447-450.

[35] Y. Nishihara, K. J. Deck, M. Shang, T. P. Fehlner, V. A. Haggerty, L. Rheingold, Organometallics 13 (1994) 4510-4522.

[36] ADF2010.02, SCM, Theoretical Chemistry, Vrije Universiteit, Amsterdam, The Netherlands, http://www.scm.com.

[37] G.teVelde, F. M. Bickelhaupt, E. J. Baerends, S.J. A.van Gisbergen, C. Fonseca Guerra, J. G. Snijders, T. Ziegler, J. Comput. Chem. 22 (2001) 931-967.

[38] S. H. Vosko, L. Wilk, M. Nusair, Can. J. Phys., 58 (1980) 1200-1211.

[39] A. D. Becke, J. Chem. Phys. 84 (1986) 4524-4529.

[40] A. D. Becke, Phys. Rev. A 38 (1986) 3098-3100.

[41] J. P. Perdew, Phys. Rev. B 33 (1986) 8822-8824.

[42] L. Versluis, T. Ziegler, J. Chem. Phys. 88 (1988) 322-329.

[43] E. van Lenthe, E. J. Baerends, J. G. Snijders, J. Chem. Phys. 99 (1993) 4597-4610.

[44] E. van Lenthe, E. F. Baerends, J. G. Snijders, J. Chem. Phys. 101 (1994) 9783-9792.

[45] E. van Lenthe, R. van Leeuwen, E. J. Baerends, J. G. Snijders, Int. J. Quantum. Chem. 57 (1996) 281-293.

[46] A. D. Becke, Phys. Rev. A, 38 (1988) 3098-3100.

[47] C. Lee, W. Yang, R. G. Parr, Phys. Re**v.** B 37 (1988) 785-789.

[48] A. D. Becke, J. Chem. Phys., 98 (1993) 5648-5652.

[49] F. London, J. Phys. Radium 27 (1937) 397-409.

[50] R. Ditchfield, Mol. Phys. 27 (1974) 789-807.

[51] K. Wolinski, J. F. Hinton, P. Pulay, J. Am. Chem. Soc. 112 (1990) 8251-8260.

[52] K. Friedrich, G. Seifert, G. Grossmann, Z. Phys. D, 17 (1990) 45-46.

[53] G Schreckenbach, T. Ziegler, J. Phys. Chem. 99 (1995) 606-611.

[54] G. Schreckenbach, T. Ziegler, Int. J. Quantum. Chem. 61 (1997) 899-918.

[55] G. Schreckenbach, T. Ziegler, Int. J. Quantum. Chem. 60 (1996) 753-766.

[56] S. K. Wolff, T. Ziegler, J. Chem. Phys. 109 (1998) 895-905.

[57] S. K. Wolff, T. Ziegler, E. van Lenthe, E. J. Baerends, J. Chem. Phys. 110 (1999) 7689-7698.

[58] T. P. Fehlner, Collect. Czech. Chem. Commun. 64 (1999) 767-782.

[59] S. K. Bose, K. Geetharani, V. Ramkumar, S. M. Mobin, S. Ghosh, Chem. Eur. J. 15 (2009) 13483-13490.

[60] J. Emsley, The Elements, Oxford University Press, Oxford, 3rd Ed., 1998.

[61] K. J. Deck, Y. Nishihara, M. Shang, T. P. Fehlner, J. Am. Chem. Soc. 116 (1994) 8408-8409.

[62] S. K. Bose, S. Ghosh, B. C. Noll, J.-F. Halet, J.-Y. Saillard, A. Vega, Organometallics 26 (2007) 5377-5385.

[63] S. Ghosh, M. Shang, T. P. Fehlner, J. Organomet. Chem., 614-615 (2000) 92-98.

[64] M. David Curtis, W. M. Butler, J. Organomet. Chem. 155 (1978) 131-145.

[65] K. Wade, J. Chem. Soc. D. (1971) 792-793.

[66] K. Wade, Adv. Inorg. Chem. Radiochem. 18 (1976) 1-66.

[67] K. Wade, in Transition Metal Clusters, B. F. G. Johnhson (ed.), Wiley, Chichester, 1980, pp. 193–264.

[68] D.M.P. Mingos, Nature Phys. Sci. 236 (1972) 99-102.

[69] D. M. P. Mingos, Acc. Chem. Res. 17 (1984) 311-319.

[70] D. M. P. Mingos, D. J. Wales, Introduction to Cluster Chemistry, Prentice-Hall, Englewood Cliffs, 1990.

[71] R. B. King, Inorg. Chem. 45 (2006) 8211-8216.

[72] R. B. King, S. Ghosh, Theor. Chem. Acc. 131 (2012) 1087.

[73] J.-F. Halet, J.-Y. Saillard, in: J. Reedijk, K. Poeppelmeier (eds.), Comprehensive Inorganic Chemistry II, Elsevier, Oxford, 2013 vol. 9: Theory and Methods (S. Alvarez, volume ed.), p. 869-885.

[74] D. M. Hoffman, R. Hoffmann, C. R. Fisel, J. Am. Chem. Soc. 104 (1982) 3858-3875.

[75] J. Autschbach, T. Ziegler, in: Encyclopedia of Nuclear Magnetic Resonance, Vol. 9, Advances in NMR, John Wiley and Sons, Chichester, 2002, pp. 306-323.

Table 1

Selected bond parameters (Å) for the compounds $(CpM)_2(B_2H_6)_2$ (**1** M = V; **2** M = Nb; **3** M = Ta) and $(Cp^*M)_2(B_2H_6)_2$ (**1'** M = V; **2'** M = Nb; **3'** M = Ta; **4** M = Cr; **5** M = Mo; **6** M = W) (Cp = η^5-C_5H_5; Cp* = η^5-C_5Me_5) optimized at the BP86/TZ2P all-electron ZORA level and corresponding experimental X-ray values [59] where available.

Cmpd.	**1** Exp.	**1** BP86/ TZ2P/ SC	**1'** BP86/ TZ2P/ SC	**2** Exp.	**2** BP86/ TZ2P/SC	**2'** BP86/ TZ2P/S C	**3'** Exp.	**3** BP86/ TZ2P/S C	**3'** BP86/ TZ2P/SC	**4** BP86/ TZ2P/S C	**5** BP86/ TZ2P/SC	**6** BP86/ TZ2P/SC
M1-M2	2.787(2)	2.735	2.735	2.948(16)	2.954	2.95	2.933(4)	2.943	2.941	2.760	2.900	2.909
M1-B3	2.295(7)	2.269	2.271	2.410(12)	2.405	2.409	2.387(13)	2.385	2.386	2.291	2.414	2.395
M1-B4	2.301(6)	2.269	2.273	2.421(11)	2.404	2.410	2.363(15)	2.384	2.385	2.291	2.413	2.398
M1-B5	2.285(6)	2.269	2.273	2.421(11)	2.404	2.409	2.369(15)	2.387	2.387	2.291	2.414	2.407
M1-B6	2.284(5)	2.27	2.271	2.410(12)	2.405	2.408	2.374(12)	2.388	2.388	2.292	2.414	2.406
M2-B3	2.285(6)	2.269	2.273	2.414(11)	2.404	2.410	2.369(15)	2.387	2.387	2.291	2.413	2.407
M2-B4	2.284(5)	2.27	2.271	2.422(11)	2.405	2.409	2.374(12)	2.388	2.388	2.292	2.414	2.406
M2-B5	2.295(7)	2.269	2.271	2.422(11)	2.405	2.408	2.387(13)	2.385	2.386	2.291	2.414	2.395
M2-B6	2.301(6)	2.269	2.273	2.414(11)	2.404	2.409	2.363(15)	2.384	2.385	2.291	2.414	2.398
B3-B4	1.734(7)	1.752	1.750	1.819(19)	1.785	1.785	1.751(3)	1.773	1.772	1.671	1.690	1.686
B5-B6	1.734(7)	1.752	1.750	1.819(19)	1.785	1.786	1.751(3)	1.773	1.772	1.671	1.690	1.686

Table 2

Selected bond parameters (Å) for the compounds $(Cp^*Cr)_2B_4H_8$ (**10**), $(Cp^*Cr(CO))_2B_4H_6$ (**11**) and $(Cp^*Cr)_2B_4H_{10}$ (**12**) optimized at the BP86/TZ2P all electron ZORA level with corresponding experimental X-ray values where available.

Compound	**10** Exp.	**10** BP86/TZ2P/SC	**11** Exp.	**11** BP86/TZ2P/SC	**12** BP86/TZ2P/SC
Cr1-Cr2	2.870(2)	2.548	2.792(1)	2.764	2.736
Cr1-B3	2.13(2)	2.18	2.16(1)	2.189	2.196
Cr1-B4	2.01(2)	2.171	2.13(1)	2.171	2.164
Cr1-B5	2.01(2)	2.17	2.11(1)	2.148	2.164
Cr1-B6	2.11(2)	2.178	2.17(1)	2.169	2.190
Cr2-B3	2.15(2)	2.18	2.16(1)	2.170	2.194
Cr2-B4	2.02(1)	2.173	2.13(1)	2.149	2.162
Cr2-B5	2.04(2)	2.172	2.11(1)	2.171	2.161
Cr2-B6	2.12(2)	2.180	2.17(1)	2.189	2.196
B3-B4	1.75(3)	1.735	1.66(2)	1.701	1.701
B4-B5	1.75(3)	1.637	1.63(2)	1.652	1.639
B5-B6	1.61(3)	1.735	1.66(2)	1.702	1.702

Table 3

DFT BP86/TZ2P and B3LYP/TZ2P computed (scalar/spin orbit ZORA) and experimental NMR chemical shifts δ (ppm) for the compounds $(CpM)_2(B_2H_6)_2$ (**1** M = V Cp = C_5H_5; **2** M = Nb, Cp = C_5H_5; **3'** M = Ta, Cp = C_5Me_5).

Compound	**1**					**2**					**3'**				
	Exp.	BP86/ TZ2P/SC	BP86/ TZ2P/ SO	B3LYP /TZ2P/ SC	B3LYP /TZ2P/ SO	Exp.	BP86/ TZ2P/ SC	BP86/ TZ2P/ SO	B3LYP/T Z2P/SC	B3LYP/ TZ2P/ SO	Exp.	BP86/ TZ2P/ SC	BP86/ TZ2P/SO	B3LYP/T Z2P/SC	B3LYP/ TZ2P/ SO
^{11}B NMR															
B3	1.7	5.6	5.9	19.2	19.5	1.7	-6.1	-4.1	0.6	2.2	-4.0	-18.9	-11.2	-13.9	-7.0
B4	1.7	5.6	5.9	19.2	19.5	1.7	-6.1	-4.1	0.6	2.2	-4.0	-18.9	-11.3	-13.9	-7.1
B5	1.7	5.6	5.9	19.2	19.5	1.7	-6.1	-4.1	0.6	2.2	-4.0	18.9	-11.2	-13.9	-7.0
B6	1.7	5.6	5.9	19.2	19.5	1.7	-6.1	-4.1	0.6	2.2	-4.0	18.9	-11.3	-13.9	-7.1
^{1}H NMR															
H9	3.4	2.7	3.1	3.0	3.5	4.1	2.4	3.3	2.5	3.3	4.4	1.6	3.7	1.7	3.4
H10	3.4	2.7	3.1	3.0	3.5	4.1	2.4	3.2	2.5	3.3	4.4	1.6	3.7	1.7	3.4
H15	3.4	2.7	3.1	3.0	3.5	4.1	2.4	3.2	2.5	3.3	4.4	1.6	3.7	1.7	3.4
H16	3.4	2.7	3.1	3.0	3.5	4.1	2.4	3.3	2.5	3.3	4.4	1.6	3.7	1.7	3.4
H12	-9.7	-10.3	-10.5	-10.8	-11.1	-10.1	-10.0	-10.8	-10.3	-10.9	-10.5	-10.2	-12.5	-10.5	-11.7
H8	-9.7	-9.9	-10.1	-10.4	-10.6	-10.1	-9.8	-10.4	-10.0	-10.6	-10.5	-10.2	-12.5	-10.5	-11.6
H13	-9.7	-9.9	-10.1	-10.4	-10.6	-10.1	-9.8	-10.4	-10.0	-10.6	-10.5	-10.6	-12.8	-10.8	-11.8
H17	-9.7	-10.3	-10.5	-10.8	-11.1	-10.1	-10.0	-10.8	-10.3	-10.9	-10.5	-10.6	-12.8	-10.8	-11.9
H7	-9.7	-9.9	-10.1	-10.4	-10.6	-10.1	-9.8	-10.5	-10.1	-10.5	-10.5	-10.6	-12.8	-10.8	-11.8
H11	-9.7	-10.3	-10.5	-10.8	-11.1	-10.1	-10.0	-10.5	-10.3	-10.7	-10.5	-10.6	-12.8	-10.8	-11.9
H18	-9.7	-10.3	-10.5	-10.8	-11.1	-10.1	-10.0	-10.5	-10.3	-10.7	-10.5	-10.2	-12.5	-10.5	-11.7
H14	-9.7	-9.9	-10.1	-10.4	-10.6	-10.1	-9.8	-10.5	-10.1	-10.5	-10.5	-10.2	-12.5	-10.5	-11.6

CpH	5.4	5.3	5.4	5.4	5.4	5.7	6.0	6.0	5.9	6.0	2.26	2.0	2.2	2.0	2.1
^{13}C NMR															
C_{Cp}	97.8	91.6	91.5	95.1	95.1	97.2	99.7	99.6	102.6	103.6	109.6	113.4	113.3	116.9	116.5
C_{Me}	-	-	-	-	-	-	-	-	-	-	13.5	10.3	10.8	10.6	11.3

Table 4

DFT BP86/TZ2P and B3LYP/TZ2P computed (scalar/spin orbit ZORA) and experimental NMR chemical shifts δ (ppm) for the compounds $(Cp^*M)_2(B_2H_6)_2$ (**4** M = Cr; **5** M = Mo; **6** M = W).

Cmpd.	**4**				**5**					**6**				
Atom	BP86/ TZ2P/ SC	BP86/ TZ2P/ SO	B3LYP /TZ2P/ SC	B3LYP/ TZ2P/SO	Exp.	BP86/ TZ2P/ SC	BP86/ TZ2P/ SO	B3LYP/ TZ2P/SC	B3LYP/ TZ2P/SO	Exp.	BP86/ TZ2P/ SC	BP86/T Z2P/SO	B3LYP/ TZ2P/SC	B3LYP/ TZ2P/SO
^{11}B NMR														
B3	-65.5	-66.9	-61.2	-62.9	-58.6	-64.2	-65.8	-60.5	-62.8	-53.9	-68.2	-70.7	-63.7	-67.5
B4	-65.7	-67.1	-61.3	-63.1	-58.6	-64.3	-65.8	-60.7	-63.0	-53.9	-68.5	-71.2	-64.0	-67.9
B5	-65.5	-66.9	-61.2	-62.9	-58.6	-64.2	-65.7	-60.6	-62.9	-53.9	-68.2	-70.7	-63.7	-67.5
B6	-65.7	-67.1	-61.3	-63.1	-58.6	-64.0	-65.6	-60.4	-62.6	-53.9	-68.5	-71.2	-64.0	-67.9
^{1}H NMR														
H9	-0.8	-0.8	-1.2	-2.0	0.6	-0.1	-1.4	-0.2	-1.5	0.3	-0.2	-3.0	-0.3	-3.2
H10	-0.9	-0.9	-1.2	-2.0	0.6	-0.2	-1.3	-0.2	-1.5	0.3	-0.2	-3.0	-0.3	-3.2
H15	-0.8	-0.8	-1.2	-2.0	0.6	-0.1	-1.3	-0.2	-1.5	0.3	-0.2	-3.0	-0.3	-3.2
H16	-0.9	-0.9	-1.2	-2.0	0.6	-0.1	-1.3	-0.1	-1.4	0.3	-0.2	-3.0	-0.3	-3.2
H12	-14.8	-16.0	-16.6	-18.0	-12.4	-10.7	-12.5	-11.3	-13.2	-10.2	-9.4	-15.0	-9.8	-14.6
H8	-14.2	-15.4	-16.1	-17.5	-12.4	-10.4	-12.6	-11.1	-13.0	-10.2	-9.6	-15.3	-10.1	-14.9
H13	-14.2	-15.4	-16.1	-17.5	-12.4	-10.3	-12.5	-11.1	-13.0	-10.2	-10.4	-16.1	-10.7	-15.4
H17	-14.9	-16.1	-16.5	-17.9	-12.4	-10.6	-12.6	-11.3	-13.1	-10.2	-10.0	-15.7	-10.4	-15.1
H7	-14.2	-15.4	-16.1	-17.5	-12.4	-10.4	-12.5	-11.1	-13.1	-10.2	-10.4	-16.1	-10.7	-15.4
H11	-14.9	-16.1	-16.5	-17.9	-12.4	-10.7	-13.1	-11.3	-13.3	-10.2	-10.0	-15.7	-10.4	-15.1
H18	-14.8	-16.0	-16.6	-18.0	-12.4	-10.6	-13.0	-11.2	-13.3	-10.2	-9.4	-15.0	-9.8	-14.6
H14	-14.2	-15.4	-16.1	-17.5	-12.4	-10.34	-12.5	-11	-13.0	-10.2	-9.6	-15.3	-10.1	-14.9

CpH	0.6	0.7	0.7	0.7	1.4	1.4	1.4	1.44	1.7	1.5	1.7	1.5	1.7
^{13}C NMR													
C_{Me}					8.5	8.4	8.9	9.0		8.8	9.8	9.4	10.7
C_{Cp}			108.3	108.1	108.7	108.4	111.8	111.5		103.3	103.6	106.1	106.0

Table 5

DFT BP86/TZ2P and B3LYP/TZ2P computed (scalar/spin orbit ZORA) and experimental NMR chemical shifts δ (ppm) for the compounds $(Cp^*Cr)_2B_4H_8$ (**10**), $(Cp^*Cr)_2B_4H_6(CO)_2$ (**11**), and $(Cp^*Cr)_2B_4H_{10}$ (**12**).

Cmpd.	**10**					**11**						**12**				
	Exp.	BP86/TZ2P/SC	BP86/TZ2P/SO	B3LYP/TZ2P/SC	B3LYP/TZ2P/SO		Exp.	BP86/TZ2P/SC	BP86/TZ2P/SO	B3LYP/TZ2P/SC	B3LYP/TZ2P/SO		BP86/TZ2P/SC	BP86/TZ2P/SO	B3LYP/TZ2P/SC	B3LYP/TZ2P/SO
B3	34.3	15.9	16.7	22.5	19.5	B3	63.9	59.4	60.6	74.5	75.1	B3	36.6	36.3	46.2	46.0
B4	126.5	22.4	21.6	-18.0	-25.0	B4	34.9	22.6	22.9	34.0	33.9	B4	32.4	31.9	53.1	53.1
B5	126.5	22.2	21.5	-18.7	-22.7	B5	34.9	22.5	21.8	33.4	33.2	B5	33.6	33.7	54.7	54.8
B6	34.3	16.6	16.5	22.5	19.4	B6	63.9	59.0	58.4	73.5	73.4	B6	37.2	38.0	47.2	47.5
H7	8.5	5.8	5.8	8.0	8.5	H7	5.2	5.0	5.5	5.0	5.5	H7	4.2	4.6	3.8	4.4
H8	3.3	2.1	1.6	-0.1	-6.9	H8	2.5	2.2	2.2	2.4	2.1	H8	3.5	3.5	4.3	4.3
H9	3.3	2.1	1.7	0.0	-6.0	H9	2.5	2.2	1.9	2.5	2.3	H9	3.5	3.4	4.6	4.5
H10	8.5	5.8	5.6	8.1	8.6	H10	5.2	5.0	5.1	5.5	5.9	H10	4.1	4.3	4.0	4.5
H11	-3.9	-8.2	-9.1	-31.6	-40.8	H11	-12.7	-12.8	-12.9	-15.1	-15.4	H11	-12.4	-12.3	-14.5	-14.6
H12	-3.9	-10.4	-11.4	-38.9	-47.0	H12	-12.7	-12.8	-14.3	-15.2	-16.3	H12	-13.2	-13.1	-15.5	-15.6
H13	-3.9	-9.7	-11.6	-37.3	-45.8	H_{Cp}	1.8	1.3	1.3	1.6	1.6	H13	-13.1	-14.7	-15.4	-16.6
H14	-3.9	-8.7	-10.5	-32.8	-42.6							H14	-12.5	-14.0	-14.7	-15.7
H_{Cp}	1.94	1.0	1.1	0.8	1.1	C_{Me}	104.6	107.8	107.9	108.1	108.2	H15	-0.2	-0.7	2.8	3.0
						C_{Cp}	9.5	10.4	10.4	10.2	10.4	H16	-0.7	-1.3	2.4	2.6
C_{Me}	108.7	101.2	101.1	104.3	103.5	C_{CO}	237.1	226.4	224.6	245.5	243.0	H_{Cp}	1.3	1.3	0.8	0.8
C_{Cp}	12.4	7.9	7.9	6.2	4.6	C_{CO}	237.1	226.2	224.4	246.0	243.5	C_{Me}	105.7	105.6	105.7	105.7
												C_{Cp}	10.4	10.4	11.1	11.4

Structural, electronic and magnetic properties of some early vs late transition dimetallaborane clusters - A theoretical investigation

Kandasamy Bharathi[a], Lalshab Beerma[a], Chinnasamy Santhi[a], Bellie Sundaram Krishnamoorthy[a,b,*] and Jean-François Halet[b,*]

[a]*Department of Chemistry, Vivekanandha College of Arts and Sciences for Women (Autonomous), Elayampalayam, Tiruchengode, 600 036, India*

[b]*Institut des Sciences Chimiques de Rennes, UMR 6226 CNRS-Université de Rennes 1, Avenue du Général Leclerc, 35042 Rennes Cédex, France*

Highlights

- The strength of DFT methods in analyzing the electronic and magnetic properties of a series of dimetallaboranes is demonstrated
- ^{11}B chemical shifts are well reproduced at the DFT-GIAO BP86/TZ2P level for first-row transition metal compounds
- B3LYP/TZ2P/SO level is necessary for second- and third-row transition metal compounds

Supplementary material

Structural, electronic and magnetic properties of some early vs late transition dimetallaborane clusters - A theoretical investigation

Kandasamy Bharathi[a], Lalshab Beerma[a], Chinnasamy Santhi[a], Bellie Sundaram Krishnamoorthy[a,b,*] and Jean-François Halet[b,*]

[a]*Department of Chemistry, Vivekanandha College of Arts and Sciences for Women (Autonomous), Elayampalayam, Tiruchengode, 600 036, India*

[b]*Institut des Sciences Chimiques de Rennes, UMR 6226 CNRS-Université de Rennes 1, Avenue du Général Leclerc, 35042 Rennes Cédex, France*

Table ST1

Selected bond (Å) and angle (°) parameters for the compounds $(Cp^*M)_2B_5H_9$ (**7** M = Cr; **8** M = Mo; **9** M = W) optimized at the BP86/TZ2P all-electron ZORA level with corresponding experimental X-ray values.

Compound	**7**	**7**	**8**	**8**	**9**	**9**
	Exp.	BP86/TZ2P/SC	Exp.	BP86/TZ2P/SC	Exp.	BP86/TZ2P/SC
M15-M16	2.625(9)	2.592	2.809(6)	2.810	2.817(8)	2.835
M15-B1	2.193(7)	2.202	2.320(4)	2.327	2.270(2)	2.322

M15-B2	2.119(6)	2.124	2.214(4)	2.231	2.220(2)	2.240
M15-B3	2.110(5)	2.113	2.181(4)	2.213	2.170(2)	2.213
M15-B4	2.120(5)	2.124	2.209(4)	2.230	2.200(2)	2.238
M15-B5	2.206(6)	2.204	2.322(4)	2.326	2.300(2)	2.321
M16-B1	2.200(5)	2.203	2.322(4)	2.327	2.290(2)	2.322
M16-B2	2.106(5)	2.124	2.211(4)	2.234	2.220(2)	2.240
M16-B3	2.108(5)	2.114	2.176(4)	2.210	2.170(2)	2.213
M16-B4	2.107(5)	2.124	2.216(4)	2.232	2.230(2)	2.238
M16-B5	2.200(6)	2.203	2.312(4)	2.325	2.317(14)	2.321
B1-B2	1.696(10)	1.720	1.732(6)	1.758	1.700(3)	1.746
B2-B3	1.669(9)	1.681	1.715(6)	1.722	1.730(2)	1.721
B3-B4	1.661(9)	1.681	1.712(7)	1.723	1.680(2)	1.721
B4-B5	1.665(11)	1.719	1.735(7)	1.759	1.730(2)	1.746
$B\text{-}B_{(average)}$	1.673	1.700	1.724	1.741	1.710	1.734
$M\text{-}B_{(average)}$	2.147	2.154	2.248	2.266	2.239	2.267

Table ST2

Selected bond parameters (Å, °) for the compounds $(Cp^*Cr)_2B_4H_8$ (**10**), $(Cp^*Cr(CO))_2B_4H_6$ (**11**) and $(Cp^*Cr)_2B_4H_{10}$ (**12**) optimized at the BP86/TZ2P all electron ZORA level with corresponding experimental X-ray values where available.

Compound	**10** Exp.	**10** BP86/TZ2P/SC	**11** Exp.	**11** BP86/TZ2P/SC	**12** BP86/TZ2P/SC
Cr1-H13	na	1.682	na	1.685[a]	1.667
Cr1-H12	na	1.678	na	1.685[b]	1.662
Cr2-H14	na	1.683	-	-	1.661
Cr2-H11	na	1.686	-	-	1.664
B3-H13	na	1.294	na	1.321[c]	1.331
B6-H12	na	1.296	na	1.321	1.334
B3-H14	na	1.292	-	-	1.335
B6-H11	na	1.292	-	-	1.333
B3-H7	na	1.207	na	1.202	1.208
B4-H8	na	1.206	na	1.202	1.206
B5-H9	na	1.206	na	1.204	1.207
B6-H10	na	1.208	na	1.202	1.208
Cr-C/H	-	-	1.817(8)	1.8432	1.5854

Cr-C/H	na	na	na	1.843	1.5794
B3-B4-B5	111(1)	123.1	120.3(8)	120.28	121.8
B4-B5-B6	113(1)	123.1	-	120.31	121.78

[a] Cr1-H11. [b] Cr2-H12. [c] B3-H11. na = not available.

Table ST3

Selected bond parameters (Å) for the compounds $(Cp^*M)_2B_3H_7$ (**15** M = Co; **16** and **16b** M = Rh; **17** M = Ir) optimized at the BP86/TZ2P all-electron scalar ZORA level with corresponding experimental X-ray values where available.

Compd	**15**	**15**		**16**	**16**	**17**		**16b**
	Exp.	BP86/TZ2P/ SC		Exp.	BP86/TZ2P/SC	BP86/TZ2P/ SC		BP86/TZ2P/S C
Co11-B1	-	2.137	M1-M2	2.6892(3)	2.74	2.773	Rh1-Rh2	2.744
Co11-B2	-	2.022	M1-B3	2.308(3)	2.342	2.311	Rh1-B3	2.375
Co11-B3	1.986(5)	2.136	M1-B5	2.292(4)	2.333	2.304	Rh1-B5	2.096
Co12-B1	-	2.138	B3-B4	1.841(5)	1.827	1.858	B3-B4	1.822
Co12-B2	1.980(5)	2.022	B4-B5	1.838(5)	1.829	1.861	B4-B5	1.826

Co12-B3	-	2.136	B3-H6	1.324(4)	1.210	1.204	B3-H6	1.207
B1-B2	1.733(8)	1.754	B4-H7	1.105(3)	1.202	1.202	B4-H7	1.203
B2-B3	1.674(9)	1.752	B5-H8	1.096(4)	1.210	1.204	B5-H8	1.201
B1-H4	1.05(7)	1.210	M1-H9	1.7905(2)	1.691	1.672	Rh1-H9	1.729
B2-H5	0.97(4)	1.207	B3-H9	1.135(3)	1.351	1.429	B3-H9	1.315
B3-H6	1.19(6)	1.210	B3-H10	1.465(3)	1.372	1.382	B3-H10	1.359
B1-H7	1.27(5)	1.319	B4-H10	1.318(4)	1.32	1.324	B4-H10	1.322
Co11-H7	1.37(5)	1.644	B4-H11	1.270(4)	1.317	1.318	B4-H11	1.299
B1-H9	1.42(5)	1.318	B5-H11	1.256(3)	1.375	1.391	B5-H11	1.397
Co12-H9	1.50(5)	1.645	B5-H12	1.345(3)	1.353	1.431	Rh2-H12	1.754
B3-H8	1.29(4)	1.320	M1-H12	1.7239(2)	1.691	1.672	Rh1-H12	1.710
Co11-H8	1.67(5)	1.642	M2-B3	2.062(3)	2.098	2.096	Rh2-B3	2.133
B3-H10	1.18(5)	1.320	M2-B4	2.061(4)	2.082	2.091	Rh2-B4	2.117
Co12-H10	1.54(5)	1.642	M2-B5	2.075(4)	2.095	2.088	Rh2-B5	2.110

Table ST4

DFT calculated (BP86/TZ2P all electron scalar ZORA level) energies of the HOMO and LUMO (eV) and HOMO-LUMO gaps (ΔE, eV) for the complexes **1-17**.

Compound	Energy (eV)	$E_{(LUMO)}$ (eV)	$E_{(HOMO)}$ (eV)	ΔE (eV)
$(CpV)_2(B_2H_6)_2$ (**1**)	-209.9264	-3.075	-4.651	1.576
$(CpNb)_2(B_2H_6)_2$(**2**)	-213.3141	-2.677	-4.441	1.764
$(CpTa)_2(B_2H_6)_2$ (**3**)	-212.0582	-2.528	-4.424	1.896
$(Cp^*V)_2(B_2H_6)_2$ (**1'**)	-373.8117	-2.570	-4.096	1.526
$(Cp^*Nb)_2(B_2H_6)_2$ (**2'**)	-377.0392	-2.199	-3.91	1.711
$(Cp^*Ta)_2(B_2H_6)_2$ (**3'**)	-375.7596	-2.096	-3.964	1.868
$(Cp^*Cr)_2(B_2H_6)_2$ (**4**)	-373.6802	-2.366	-3.072	0.706
$(Cp^*Mo)_2(B_2H_6)_2$ (**5**)	-376.0322	-1.529	-2.944	1.415
$(Cp^*W)_2(B_2H_6)_2$ (**6**)	-376.0691	-1.470	-2.976	1.506
$(Cp^*Cr)_2B_5H_9$ (**7**)	-370.646	-2.688	-4.674	1.986
$(Cp^*Mo)_2B_5H_9$ (**8**)	-372.9805	-2.248	-4.661	2.413
$(Cp^*W)_2B_5H_9$ (**9**)	-373.2871	-2.158	-4.733	2.575
$(Cp^*Cr)_2B_4H_8$ (**10**)	-359.0791	-2.613	-3.259	0.646
$(Cp^*Cr(CO))_2B_4H_6$ (**11**)	-384.4594	-2.658	-4.292	1.634

$(Cp^*Cr)_2B_4H_{10}$ (**12**)	-366.6190	-2.389	-4.599	2.210
$(Cp^*Cr)_2B_4H_{10}$ (**13**)	-359.3630	-2.539	-4.110	1.571
$(Cp^*Cr)_2(B_2H_4)_2$(**14**)	-358.7050	-3.308	-4.286	0.978
$(Cp^*Co)_2B_3H_7$(**15**)	-346.7935	-2.411	-3.569	1.158
$(Cp^*Rh)_2B_3H_7$ (**16**)	-344.4439	-1.958	-3.965	2.007
$(Cp^*Rh)_2B_3H_7$(**16b**)	-344.4327	-1.982	-3.846	1.864
$(Cp^*Ir)_2B_3H_7$ (**17**)	-347.6643	-1.337	-3.951	2.614

Table ST5

DFT BP86/TZ2P and B3LYP/TZ2P computed (Scalar/spin orbit ZORA) and experimental NMR chemical shifts δ (ppm) for the compounds $(Cp^*M)B_5H_9$ (**7** M = Cr; **8** M = Mo; **9** M = W).

	7					**8**					**9**				
	Exp.	BP86/ TZ2P/ SC	BP86/TZ2P/SO	B3LYP/ TZ2P/ SC	B3LYP/TZ2P/ SO	Exp.	BP86/ TZ2P/ SC	BP86/ TZ2P/ SO	B3LYP /TZ2P/ SC	B3LYP/TZ2P/ SO	Exp.	BP86/ TZ2P/ SC	BP86/ TZ2P/ SO	B3LYP/ TZ2P/SC	B3LYP/TZ2P/ SO
^{11}B NMR															
B1	25.0	28.5	28.7	46.4	46.2	28.4	21.3	23.0	30.0	31.3	26.8	15.0	22.0	21.84	28.0
B2	91.5	78.6	77.8	116.4	116.2	65.6	50.6	52.7	66.5	67.9	46.9	31.8	38.6	43.73	49.2
B3	86.2	68.2	67.5	95.2	94.9	65.6	47.9	49.3	61.8	62.8	49.2	35.8	42.1	46.98	51.7
B4	91.5	78.4	78.8	116.3	116.3	65.6	51.1	52.6	67.2	68.6	46.9	32.3	39.1	44.17	49.6
B5	25.0	28.4	29.1	47.2	47.1	28.4	21.6	23.0	30.2	31.6	26.8	15.0	22.0	21.86	28.0
^{1}H NMR															
H6	4.6	4.3	4.5	5.1	5.4	5.01	3.9	5.5	4.2	4.7	6.42	3.6	5.3	3.71	5.4
H7	6.7	5.2	5.5	7.1	7.6	5.61	4.0	5.0	4.5	5.5	6.42	3.0	5.4	3.33	5.7
H8	3.2	3.14	3.2	3.8	3.9	3.43	2.4	2.9	2.5	3.0	3.94	1.7	3.2	1.82	3.2
H9	6.7	5.2	5.6	6.8	7.4	5.61	4.1	5.0	4.6	5.6	6.42	3.0	5.4	3.31	5.7

H10	4.6	4.3	4.7	5.1	5.4	5.01	3.8	4.5	4.1	4.7	6.42	3.5	5.3	3.68	5.3
H11	-6.2	-7.1	-7.9	-4.9	-5.3	-6.84	-7.2	-8.3	-7.0	-7.6	-8.2	-7.2	-10.1	-7.03	-8.9
H12	-6.2	-7.0	-7.6	-4.8	-5.2	-6.84	-7.2	-8.2	-7.0	-7.6	-8.2	-7.2	-10.1	-7.03	-8.9
H13	-6.2	-7.1	-8.1	-4.8	-5.3	-6.84	-7.3	-8.3	-7.1	-7.7	-8.2	-7.3	-10.2	-7.13	-9.0
H14	-6.2	-7.0	-8.3	-4.7	-5.3	-6.84	-7.3	-8.2	-7.1	-7.7	-8.2	-7.3	-10.2	-7.13	-9.0
H_{Cp*}	1.81	1.9	1.9	1.4	1.4	1.93	1.7	1.9	1.7	1.7	2.08	1.6	2.0	1.45	1.9
^{13}C NMR															
C_{Cp}	108.1	106.6	106.5	109.4	109.3	na	108.8	107.9	-	111.8	na	107.4	107.5	110.7	110.5
C_{Me}	12.9	9.3	9.2	9.6	9.8	na	10.7	10.0	-	10.5	na	9.1	9.2	9.5	9.9

Table ST6

DFT BP86/TZ2P and B3LYP/TZ2P computed (scalar/spin orbit ZORA) and experimental NMR chemical shifts δ (ppm) for the compounds $(Cp^*M)_2B_3H_7$ (**15** M = Co; **16** M = Rh; **16b** M = Rh).

Cmpd.	**15**					**16**					**16b**				
	Exp.	BP86/TZ2P/SC	BP86/TZ2P/SO	B3LYP/TZ2P/SC	B3LYP/TZ2P/SO	Exp.	BP86/TZ2P/SC	BP86/TZ2P/SO	B3LYP/TZ2P/SC	B3LYP/TZ2P/SO	Exp.	BP86/TZ2P/SC	BP86/TZ2P/SO	B3LYP/TZ2P/SC	B3LYP/TZ2P/SO
^{11}B NMR															
B3	-18.1	-17.1	21.0	-19.2	-25.6	na	5.3	1.0	9.6	5.3	na	-7.0	-13.4	-4.3	-12.9
B4	65.8	72.8	68.9	64.3	58.6	na	1.0	0.1	2.7	0.8	na	1.0	-0.4	3.2	1.5
B5	-18.1	-16.1	-20.6	-18.4	-24.8	na	6.4	3.9	10.4	5.0	na	52.2	47.3	56.8	48.5
^{1}H NMR															
H6	na	1.2	0.8	0.3	-0.2	3.7	3.0	2.8	2.8	2.7	2.7	2.3	1.9	2.1	1.7
H7	6.3	6.0	6.0	5.9	5.8	4.0	2.3	3.3	2.0	3.1	4.2	2.7	3.3	2.5	3.2
H8	na	1.3	0.9	0.4	-0.1	3.7	3.2	3.2	2.9	2.8	5.7	5.2	5.6	5.2	5.5
H9	-12.7	-7.6	-9.0	-11.9	-14.2	-12.0	-9.6	-11.6	-11.4	-14.3	-15.0	-11.8	-16.7	-13.9	-19.2
H10	-12.7	-7.6	-9.0	-11.6	-14.3	-3.1	-2.8	-3.6	-3.6	-4.6	-3.4	-3.1	-4.4	-4.0	-5.5
H11	-12.7	-7.6	-9.0	-11.5	-14.2	-3.1	-2.7	-3.9	-3.6	-5.0	-0.2	0.5	-0.7	-0.6	-1.9

H12	-12.7	-7.6	-9.0	-11.6	-14.3	-12.0	-9.5	-14.0	-11.3	-15.4	-14.5	-8.6	-9.8	-10.2	-14.6
H(Cp)	1.7	1.7	1.6	1.6	1.5	1.5	1.3	1.2	1.5	1.2	1.7	1.3	1.2	1.2	1.0
^{13}C NMR															
C_{Cp}	10.3	5.6	5.5	5.4	5.5	na	6.9	6.5	6.7	6.6	na	7.1	7.0	6.6	6.7
C_{Me}	89.6	94.4	94.6	93.5	94.2	na	90.3	89.9	91.5	91.0	na	86.7	85.5	86.1	84.7

Cartesian coordinates for the optimized geometries of clusters 1-17.

1

1.V	0.779443	0.561109	0.973806
2.V	-0.779443	-0.561109	-0.973806
3.B	-1.466686	0.771067	0.729884
4.B	-0.990940	-0.826116	1.270682
5.B	1.466686	-0.771067	-0.729884
6.B	0.990940	0.826116	-1.270682
7.H	-1.716783	0.883710	-0.516645
8.H	0.179198	-0.912912	1.773738
9.H	-2.453070	1.207383	1.273024
10.H	-1.712716	-1.301153	2.114297
11.H	-0.953772	-1.725220	0.358764
12.H	-0.591187	1.689946	0.907077
13.H	1.716783	-0.883710	0.516645
14.H	-0.179198	0.912912	-1.773738
15.H	2.453070	-1.207383	-1.273024
16.H	1.712716	1.301153	-2.114297
17.H	0.953772	1.725220	-0.358764
18.H	0.591187	-1.689946	-0.907077
19.C	1.055476	1.066402	3.173510
20.C	2.143318	0.251028	2.734162
21.C	2.883729	0.988652	1.760029
22.C	2.249294	2.242282	1.593323
23.C	1.121949	2.291160	2.462199
24.H	0.304603	0.793210	3.905580
25.H	2.384263	-0.741006	3.098845
26.H	3.761467	0.643003	1.226216
27.H	2.558705	3.025562	0.910263
28.H	0.431812	3.121857	2.558794
29.C	-1.055476	-1.066402	-3.173510
30.C	-2.143318	-0.251028	-2.734162
31.C	-2.883729	-0.988652	-1.760029

32.C	-2.249294	-2.242282	-1.593323
33.C	-1.121949	-2.291160	-2.462199
34.H	-0.304603	-0.793210	-3.905580
35.H	-2.384263	0.741006	-3.098845
36.H	-3.761467	-0.643003	-1.226216
37.H	-2.558705	-3.025562	-0.910263
38.H	-0.431812	-3.121857	-2.558794

2

1.Nb	1.042179	1.022764	0.000000
2.Nb	2.299335	3.695379	0.000000
3.B	2.477897	1.978290	-1.674657
4.B	0.863466	2.739795	-1.674725
5.B	2.477897	1.978290	1.674657
6.B	0.863466	2.739795	1.674725
7.H	0.428194	2.942073	-2.783185
8.H	2.590280	0.826466	-1.095148
9.H	3.437756	2.637052	-1.101211
10.H	-0.096467	2.081061	-1.101343
11.H	0.751225	3.891796	-1.095436
12.H	2.913433	1.775898	-2.782938
13.H	0.428194	2.942073	2.783185
14.H	2.590280	0.826466	1.095148
15.H	3.437756	2.637052	1.101211
16.H	-0.096467	2.081061	1.101343
17.H	0.751225	3.891796	1.095436
18.H	2.913433	1.775898	2.782938
19.C	4.097129	5.207591	0.712993
20.C	2.862626	5.747432	1.158231
21.C	2.085088	6.071069	0.000000
22.C	4.097129	5.207591	-0.712993
23.C	2.862626	5.747432	-1.158231
24.H	4.903790	4.855489	1.347222
25.H	2.563194	5.887776	2.190609

26.H	1.106197	6.537511	0.000000
27.H	4.903790	4.855489	-1.347222
28.H	2.563194	5.887776	-2.190609
29.C	1.259973	-1.352597	0.000000
30.C	0.481950	-1.030191	-1.158224
31.C	-0.753388	-0.492242	-0.712991
32.C	0.481950	-1.030191	1.158224
33.C	-0.753388	-0.492242	0.712991
34.H	2.239604	-1.817466	0.000000
35.H	0.781663	-1.170032	-2.190571
36.H	-1.560616	-0.141412	-1.347204
37.H	0.781663	-1.170032	2.190571
38.H	-1.560616	-0.141412	1.347204

3

1.Ta	-0.650502	-0.508418	-1.218255
2.Ta	0.650502	0.508418	1.218255
3.B	0.766878	-1.688233	0.299174
4.B	-0.823492	-1.354144	1.007712
5.B	-0.766878	1.688233	-0.299174
6.B	0.823492	1.354144	-1.007712
7.H	-0.907005	-0.358473	1.842791
8.H	1.755291	-0.918675	0.663246
9.H	-1.298431	-2.264090	1.640338
10.H	0.870659	-1.609813	-0.996866
11.H	-1.791879	-1.056294	0.185253
12.H	1.202829	-2.788981	0.527305
13.H	0.907005	0.358473	-1.842791
14.H	-1.755291	0.918675	-0.663246
15.H	1.298431	2.264090	-1.640338
16.H	-0.870659	1.609813	0.996866
17.H	1.791879	1.056294	-0.185253
18.H	-1.202829	2.788981	-0.527305
19.C	-2.300656	-1.958057	-2.297426

20.C	-1.027459	-2.323102	-2.797137
21.C	-0.483587	-1.196722	-3.492579
22.C	-1.441897	-0.133031	-3.431952
23.C	-2.559912	-0.606202	-2.678732
24.C	1.027459	2.323102	2.797137
25.C	0.483587	1.196722	3.492579
26.C	1.441897	0.133031	3.431952
27.C	2.559912	0.606202	2.678732
28.C	2.300656	1.958057	2.297426
29.H	-0.465429	1.172680	4.017233
30.H	1.345342	-0.844274	3.890395
31.H	3.464330	0.048475	2.460424
32.H	2.957534	2.590470	1.709490
33.H	0.542640	3.283899	2.661075
34.H	0.465429	-1.172680	-4.017233
35.H	-1.345342	0.844274	-3.890395
36.H	-3.464330	-0.048475	-2.460424
37.H	-2.957534	-2.590470	-1.709490
38.H	-0.542640	-3.283899	-2.661075

1’

1.V	0.778251	0.564673	0.972639
2.V	-0.778251	-0.564673	-0.972639
3.B	-1.470664	0.771053	0.731453
4.B	-0.996181	-0.823945	1.273353
5.B	1.470664	-0.771053	-0.731453
6.B	0.996181	0.823945	-1.273353
7.H	-1.721309	0.877116	-0.516359
8.H	0.174246	-0.904983	1.778186
9.H	-2.460736	1.212414	1.269116
10.H	-1.716222	-1.302788	2.119879
11.H	-0.952312	-1.724318	0.364523
12.H	-0.595334	1.689724	0.901249
13.H	1.721309	-0.877116	0.516359

14.H	-0.174246	0.904983	-1.778186
15.H	2.460736	-1.212414	-1.269116
16.H	1.716222	1.302788	-2.119879
17.H	0.952312	1.724318	-0.364523
18.H	0.595334	-1.689724	-0.901249
19.C	-1.112395	-2.297537	-2.459536
20.C	-1.046490	-1.063290	-3.172456
21.C	-2.140605	-0.244008	-2.728576
22.C	-2.884594	-0.987996	-1.749904
23.C	-2.246171	-2.250055	-1.584468
24.C	1.046490	1.063290	3.172456
25.C	2.140605	0.244008	2.728576
26.C	2.884594	0.987996	1.749904
27.C	2.246171	2.250055	1.584468
28.C	1.112395	2.297537	2.459536
29.C	0.086831	0.732181	4.275336
30.C	2.543916	-1.076997	3.315879
31.C	4.169952	0.562993	1.106542
32.C	2.749339	3.377186	0.732551
33.C	0.231129	3.489866	2.688321
34.C	-0.086831	-0.732181	-4.275336
35.C	-2.543916	1.076997	-3.315879
36.C	-4.169952	-0.562993	-1.106542
37.C	-2.749339	-3.377186	-0.732551
38.C	-0.231129	-3.489866	-2.688321
39.H	-0.108058	-0.345420	4.332035
40.H	0.491095	1.051509	5.249410
41.H	-0.878355	1.232460	4.133002
42.H	3.060488	-1.706093	2.581070
43.H	3.229157	-0.927462	4.165616
44.H	1.676655	-1.637697	3.684295
45.H	4.282409	0.996474	0.105628
46.H	5.030618	0.887830	1.712936
47.H	4.229394	-0.526767	1.000541
48.H	1.941428	4.058793	0.440835
49.H	3.498898	3.966167	1.284324
50.H	3.223192	3.009216	-0.185541

51.H	-0.784929	3.192919	2.974284
52.H	0.638620	4.114413	3.498987
53.H	0.155898	4.118018	1.792523
54.H	0.108058	0.345420	-4.332035
55.H	0.878355	-1.232460	-4.133002
56.H	-0.491095	-1.051509	-5.249410
57.H	-3.060488	1.706093	-2.581070
58.H	-1.676655	1.637697	-3.684295
59.H	-3.229157	0.927462	-4.165616
60.H	-4.282409	-0.996474	-0.105628
61.H	-4.229394	0.526767	-1.000541
62.H	-5.030618	-0.887830	-1.712936
63.H	-1.941428	-4.058793	-0.440835
64.H	-3.223192	-3.009216	0.185541
65.H	-3.498898	-3.966167	-1.284324
66.H	0.784929	-3.192919	-2.974284
67.H	-0.155898	-4.118018	-1.792523
68.H	-0.638620	-4.114413	-3.498987

2’

1.Nb	1.036511	1.027264	-0.006728
2.Nb	2.306385	3.690153	-0.006908
3.B	2.477391	1.974765	-1.689647
4.B	0.865426	2.742497	-1.689663
5.B	2.477627	1.975175	1.674429
6.B	0.865343	2.742435	1.674443
7.H	0.432474	2.949290	-2.801197
8.H	2.579418	0.820896	-1.111218
9.H	3.439505	2.625956	-1.113578
10.H	-0.096639	2.091396	-1.113418
11.H	0.763440	3.896471	-1.111387
12.H	2.910270	1.767783	-2.801174
13.H	0.434640	2.951021	2.786684
14.H	2.582059	0.822657	1.093905

15.H	3.440355	2.627366	1.101137
16.H	-0.097420	2.090127	1.101347
17.H	0.760850	3.894860	1.093751
18.H	2.908461	1.766780	2.786647
19.C	-0.740391	-0.484154	0.747038
20.C	-0.773060	-0.472311	-0.689059
21.C	0.461076	-1.009965	-1.169240
22.C	1.270932	-1.342013	-0.023683
23.C	0.513554	-1.027245	1.161662
24.C	4.083430	5.201363	0.747019
25.C	2.829481	5.744481	1.161647
26.C	2.072272	6.059583	-0.023669
27.C	2.882049	5.727425	-1.169248
28.C	4.116145	5.189634	-0.689070
29.C	5.221230	4.836715	1.657720
30.C	2.430755	6.065672	2.573390
31.C	0.773092	6.815537	-0.057221
32.C	5.297903	4.815872	-1.538274
33.C	2.550189	6.034751	-2.601155
34.C	2.570205	-2.097823	-0.057234
35.C	0.793000	-1.317070	-2.601175
36.C	-1.954805	-0.098567	-1.538295
37.C	0.912224	-1.348637	2.573355
38.C	-1.878251	-0.119570	1.657691
39.H	5.874681	4.079087	1.209587
40.H	5.838987	5.722608	1.874071
41.H	4.862181	4.440525	2.614763
42.H	2.886172	5.372328	3.289965
43.H	2.750185	7.084642	2.844702
44.H	1.344555	6.011193	2.711149
45.H	0.146713	6.584163	0.812311
46.H	0.957462	7.902127	-0.053976
47.H	0.190888	6.581559	-0.956106
48.H	1.472112	5.972856	-2.790368
49.H	2.876929	7.053276	-2.865592
50.H	3.043224	5.337899	-3.288688
51.H	4.987488	4.412926	-2.509368

52.H	5.927782	5.699064	-1.729447
53.H	5.925997	4.060772	-1.051268
54.H	3.196570	-1.866342	0.812282
55.H	2.386001	-3.184445	-0.053954
56.H	3.152375	-1.863796	-0.956132
57.H	1.871094	-1.255253	-2.790301
58.H	0.466165	-2.335509	-2.865804
59.H	0.300081	-0.620045	-3.288620
60.H	-1.644359	0.304478	-2.509346
61.H	-2.584626	-0.981786	-1.729570
62.H	-2.582972	0.656455	-1.051266
63.H	-2.531698	0.638037	1.209522
64.H	-2.495994	-1.005476	1.874020
65.H	-1.519256	0.276641	2.614748
66.H	0.456499	-0.655619	3.290036
67.H	0.593065	-2.367769	2.844361
68.H	1.998393	-1.293869	2.711258

3’

1.Ta	0.651235	0.505427	1.217561
2.Ta	-0.651235	-0.505427	-1.217561
3.B	-0.825323	-1.356629	1.005240
4.B	0.764463	-1.691157	0.296679
5.B	0.825323	1.356629	-1.005240
6.B	-0.764463	1.691157	-0.296679
7.H	0.867926	-1.609908	-0.999109
8.H	-1.793625	-1.054145	0.185708
9.H	1.198885	-2.795618	0.518658
10.H	-0.904659	-0.363339	1.843710
11.H	1.753448	-0.924214	0.662189
12.H	-1.303214	-2.268525	1.636301
13.H	-0.867926	1.609908	0.999109
14.H	1.793625	1.054145	-0.185708
15.H	-1.198885	2.795618	-0.518658

16.H	0.904659	0.363339	-1.843710
17.H	-1.753448	0.924214	-0.662189
18.H	1.303214	2.268525	-1.636301
19.C	-0.780100	1.202406	4.321208
20.H	-1.210816	0.198577	4.413735
21.H	-1.549901	1.855909	3.893579
22.H	-0.562696	1.566301	5.338330
23.C	1.361043	-1.171052	4.180520
24.H	0.327369	-1.524270	4.272568
25.H	1.767292	-1.057314	5.198613
26.H	1.932803	-1.960877	3.679945
27.C	3.862381	-0.127227	2.482593
28.H	4.369661	0.176360	1.559139
29.H	3.715286	-1.212667	2.439853
30.H	4.544382	0.083657	3.321664
31.C	3.246405	2.873544	1.560686
32.H	3.947096	2.315351	0.928937
33.H	3.840017	3.454992	2.283303
34.H	2.714420	3.584507	0.917252
35.C	0.393090	3.689210	2.689789
36.H	0.662275	4.194577	1.754751
37.H	0.731715	4.323623	3.523935
38.H	-0.701166	3.639888	2.734226
39.C	1.014392	2.326025	2.781504
40.C	0.470825	1.194762	3.487752
41.C	1.437604	0.127223	3.430314
42.C	2.561749	0.601447	2.670189
43.C	2.296731	1.959704	2.279016
44.C	0.780100	-1.202406	-4.321208
45.H	1.210816	-0.198577	-4.413735
46.H	1.549901	-1.855909	-3.893579
47.H	0.562696	-1.566301	-5.338330
48.C	-1.361043	1.171052	-4.180520
49.H	-0.327369	1.524270	-4.272568
50.H	-1.767292	1.057314	-5.198613
51.H	-1.932803	1.960877	-3.679945
52.C	-3.862381	0.127227	-2.482593

53.H	-4.369661	-0.176360	-1.559139
54.H	-3.715286	1.212667	-2.439853
55.H	-4.544382	-0.083657	-3.321664
56.C	-3.246405	-2.873544	-1.560686
57.H	-3.947096	-2.315351	-0.928937
58.H	-3.840017	-3.454992	-2.283303
59.H	-2.714420	-3.584507	-0.917252
60.C	-0.393090	-3.689210	-2.689789
61.H	-0.662275	-4.194577	-1.754751
62.H	-0.731715	-4.323623	-3.523935
63.H	0.701166	-3.639888	-2.734226
64.C	-1.014392	-2.326025	-2.781504
65.C	-0.470825	-1.194762	-3.487752
66.C	-1.437604	-0.127223	-3.430314
67.C	-2.561749	-0.601447	-2.670189
68.C	-2.296731	-1.959704	-2.279016

4

1.Cr	0.788578	0.555247	0.986849
2.Cr	-0.788578	-0.555247	-0.986849
3.B	-1.486228	0.731848	0.775794
4.B	-1.037541	-0.797247	1.278335
5.B	1.486228	-0.731848	-0.775794
6.B	1.037541	0.797247	-1.278335
7.H	-1.659867	0.859864	-0.501501
8.H	0.180721	-0.891164	1.710600
9.H	-2.451323	1.300123	1.233654
10.H	-1.662693	-1.405841	2.116752
11.H	-0.923260	-1.674972	0.332975
12.H	-0.562136	1.634075	0.886305
13.H	1.659867	-0.859864	0.501501
14.H	-0.180721	0.891164	-1.710600
15.H	2.451323	-1.300123	-1.233654
16.H	1.662693	1.405841	-2.116752

17.H	0.923260	1.674972	-0.332975
18.H	0.562136	-1.634075	-0.886305
19.C	-1.065616	-2.274551	-2.388229
20.C	-0.968027	-1.020447	-3.075041
21.C	-2.063459	-0.185616	-2.625598
22.C	-2.822246	-0.951630	-1.661044
23.C	-2.202871	-2.230020	-1.527809
24.C	0.968027	1.020447	3.075041
25.C	2.063459	0.185616	2.625598
26.C	2.822246	0.951630	1.661044
27.C	2.202871	2.230020	1.527809
28.C	1.065616	2.274551	2.388229
29.C	-0.002760	0.699180	4.169907
30.C	2.468452	-1.131662	3.215659
31.C	4.104309	0.534570	1.007867
32.C	2.707753	3.354564	0.676248
33.C	0.180608	3.462822	2.613847
34.C	0.002760	-0.699180	-4.169907
35.C	-2.468452	1.131662	-3.215659
36.C	-4.104309	-0.534570	-1.007867
37.C	-2.707753	-3.354564	-0.676248
38.C	-0.180608	-3.462822	-2.613847
39.H	-0.148130	-0.382242	4.272749
40.H	0.361916	1.085385	5.135583
41.H	-0.986913	1.143559	3.977519
42.H	2.992528	-1.755704	2.481325
43.H	3.143626	-0.984944	4.074039
44.H	1.597162	-1.696863	3.568482
45.H	4.179595	0.921919	-0.015537
46.H	4.966513	0.914599	1.579238
47.H	4.191960	-0.556337	0.952680
48.H	1.907188	4.053584	0.407515
49.H	3.477655	3.921424	1.223044
50.H	3.158093	2.984990	-0.252883
51.H	-0.846673	3.160238	2.849949
52.H	0.559456	4.059486	3.458565
53.H	0.144825	4.116610	1.734320

54.H	0.148130	0.382242	-4.272749
55.H	0.986913	-1.143559	-3.977519
56.H	-0.361916	-1.085385	-5.135583
57.H	-2.992528	1.755704	-2.481325
58.H	-1.597162	1.696863	-3.568482
59.H	-3.143626	0.984944	-4.074039
60.H	-4.179595	-0.921919	0.015537
61.H	-4.191960	0.556337	-0.952680
62.H	-4.966513	-0.914599	-1.579238
63.H	-1.907188	-4.053584	-0.407515
64.H	-3.158093	-2.984990	0.252883
65.H	-3.477655	-3.921424	-1.223044
66.H	0.846673	-3.160238	-2.849949
67.H	-0.144825	-4.116610	-1.734320
68.H	-0.559456	-4.059486	-3.458565

5

1.Mo	1.055657	1.045928	0.003736
2.Mo	2.285523	3.672209	0.003797
3.B	0.904816	2.717642	1.738378
4.B	2.435273	2.000285	1.738997
5.B	2.436102	1.999937	-1.730909
6.B	0.906006	2.717879	-1.731385
7.H	0.347271	2.984217	-2.772598
8.H	2.553988	0.868533	-1.065966
9.H	3.385778	2.643733	-1.085254
10.H	-0.044031	2.074109	-1.085528
11.H	0.788141	3.849886	-1.067239
12.H	2.994366	1.732854	-2.772168
13.H	0.345126	2.984671	2.778749
14.H	2.552742	0.868334	1.075453
15.H	3.384820	2.644129	1.093130
16.H	-0.044528	2.074140	1.091533
17.H	0.788729	3.850228	1.074636

18.H	2.993258	1.734275	2.780555
19.C	-0.724010	-0.348722	0.697491
20.C	-0.706961	-0.359772	-0.731272
21.C	0.569639	-0.841889	-1.171373
22.C	1.372344	-1.138630	0.012200
23.C	0.542870	-0.826382	1.174755
24.C	4.066341	5.064520	0.699154
25.C	2.799299	5.542957	1.176049
26.C	1.971307	5.857009	0.013253
27.C	2.774434	5.559544	-1.170100
28.C	4.050511	5.076630	-0.729392
29.C	5.238234	4.699140	1.560808
30.C	2.462641	5.836963	2.608139
31.C	0.685565	6.630790	0.030921
32.C	5.199243	4.720007	-1.625142
33.C	2.402951	5.866514	-2.590761
34.C	2.659118	-1.910734	0.031722
35.C	0.943313	-1.146569	-2.592013
36.C	-1.855156	-0.003316	-1.627789
37.C	0.880707	-1.122416	2.606132
38.C	-1.896311	0.016580	1.558853
39.H	-1.575449	0.463541	2.507044
40.H	-2.559256	0.732333	1.059329
41.H	-2.488423	-0.881866	1.793496
42.H	-2.531369	0.718290	-1.155422
43.H	-1.508213	0.431527	-2.572418
44.H	-2.440816	-0.904669	-1.867506
45.H	0.506933	-0.420210	-3.287451
46.H	2.029126	-1.121415	-2.735953
47.H	0.587254	-2.148290	-2.881738
48.H	3.275029	-1.681210	-0.846081
49.H	3.254568	-1.670373	0.920566
50.H	2.471677	-2.997064	0.035952
51.H	1.380602	5.813165	2.778814
52.H	2.913579	5.102633	3.285671
53.H	2.828537	6.835050	2.898117
54.H	4.917376	4.252335	2.509053

55.H	5.901692	3.983861	1.061345
56.H	5.829870	5.597920	1.795633
57.H	5.874587	3.997707	-1.152569
58.H	4.852971	4.286011	-2.570394
59.H	5.785639	5.621193	-1.863683
60.H	2.841002	5.141642	-3.286708
61.H	1.317448	5.841131	-2.736922
62.H	2.759141	6.868909	-2.877904
63.H	0.071821	6.403207	-0.848877
64.H	0.087253	6.389931	0.917753
65.H	0.874403	7.716874	0.037246
66.H	0.421702	-0.395179	3.285909
67.H	0.523704	-2.124967	2.891808
68.H	1.962210	-1.088837	2.778150

6

1.W	0.627657	0.486910	1.218354
2.W	-0.627657	-0.486910	-1.218354
3.B	-0.805137	-1.419474	0.993642
4.B	0.713784	-1.740852	0.335557
5.B	0.805137	1.419474	-0.993642
6.B	-0.713784	1.740852	-0.335557
7.H	0.850816	-1.573170	-0.968868
8.H	-1.748462	-1.030234	0.155955
9.H	1.238563	-2.814760	0.487050
10.H	-0.897702	-0.379205	1.801355
11.H	1.692725	-0.930088	0.683173
12.H	-1.394838	-2.258366	1.626306
13.H	-0.850816	1.573170	0.968868
14.H	1.748462	1.030234	-0.155955
15.H	-1.238563	2.814760	-0.487050
16.H	0.897702	0.379205	-1.801355
17.H	-1.692725	0.930088	-0.683173
18.H	1.394838	2.258366	-1.626306

19.C	-0.828397	1.187260	4.222268
20.H	-1.298114	0.198440	4.290816
21.H	-1.585146	1.887741	3.847644
22.H	-0.559155	1.500532	5.244318
23.C	1.313387	-1.214571	4.047349
24.H	0.283362	-1.567461	4.177229
25.H	1.751961	-1.078476	5.049673
26.H	1.868839	-2.015216	3.544067
27.C	3.816766	-0.151518	2.345829
28.H	4.357600	0.195980	1.457085
29.H	3.669917	-1.233595	2.244090
30.H	4.466294	0.016611	3.219853
31.C	3.207176	2.857764	1.473666
32.H	3.901174	2.301843	0.833095
33.H	3.805269	3.422010	2.205860
34.H	2.676348	3.582002	0.844516
35.C	0.363118	3.672654	2.588614
36.H	0.641504	4.184450	1.659636
37.H	0.704597	4.294017	3.431318
38.H	-0.731091	3.628211	2.628454
39.C	0.974387	2.306021	2.674888
40.C	0.384962	1.157311	3.337479
41.C	1.359638	0.063305	3.261057
42.C	2.509447	0.565943	2.518165
43.C	2.257908	1.943117	2.187767
44.C	0.828397	-1.187260	-4.222268
45.H	1.298114	-0.198440	-4.290816
46.H	1.585146	-1.887741	-3.847644
47.H	0.559155	-1.500532	-5.244318
48.C	-1.313387	1.214571	-4.047349
49.H	-0.283362	1.567461	-4.177229
50.H	-1.751961	1.078476	-5.049673
51.H	-1.868839	2.015216	-3.544067
52.C	-3.816766	0.151518	-2.345829
53.H	-4.357600	-0.195980	-1.457085
54.H	-3.669917	1.233595	-2.244090
55.H	-4.466294	-0.016611	-3.219853

56.C	-3.207176	-2.857764	-1.473666
57.H	-3.901174	-2.301843	-0.833095
58.H	-3.805269	-3.422010	-2.205860
59.H	-2.676348	-3.582002	-0.844516
60.C	-0.363118	-3.672654	-2.588614
61.H	-0.641504	-4.184450	-1.659636
62.H	-0.704597	-4.294017	-3.431318
63.H	0.731091	-3.628211	-2.628454
64.C	-0.974387	-2.306021	-2.674888
65.C	-0.384962	-1.157311	-3.337479
66.C	-1.359638	-0.063305	-3.261057
67.C	-2.509447	-0.565943	-2.518165
68.C	-2.257908	-1.943117	-2.187767

7

1.B	12.178911	6.263173	2.867862
2.B	11.158875	4.948524	3.302518
3.B	11.148522	4.279777	4.844639
4.B	12.155386	4.885691	6.046196
5.B	13.234317	6.197521	5.778931
6.H	12.097567	6.657890	1.730474
7.H	10.418972	4.494864	2.466720
8.H	10.415430	3.360131	5.089982
9.H	12.127022	4.378119	7.138463
10.H	13.908129	6.544473	6.717934
11.H	13.437289	5.993603	3.032775
12.H	11.969369	7.316496	3.597196
13.H	12.622505	7.276625	5.398074
14.H	14.089522	5.952240	4.833728
15.Cr	13.093951	4.722350	4.147991
16.Cr	11.242795	6.391877	4.857988
17.C	14.754088	3.415676	4.776306
18.C	13.592022	2.597610	4.622258
19.C	13.169274	2.678334	3.251158

20.C	14.071884	3.544873	2.561654
21.C	15.053376	4.003979	3.502396
22.C	15.574360	3.546773	6.023332
23.H	14.948252	3.487794	6.921341
24.H	16.112958	4.501214	6.056684
25.H	16.321841	2.739462	6.076899
26.C	13.034681	1.666992	5.654550
27.H	11.960998	1.501367	5.509804
28.H	13.179385	2.056249	6.668976
29.H	13.541563	0.690306	5.588898
30.C	12.091214	1.851917	2.620964
31.H	11.688273	2.331783	1.721710
32.H	11.256884	1.684564	3.312141
33.H	12.494973	0.868504	2.329425
34.C	14.050494	3.839872	1.092729
35.H	13.024460	3.889090	0.709305
36.H	14.582789	3.052485	0.536285
37.H	14.536498	4.795437	0.863199
38.C	16.251790	4.847809	3.181378
39.H	16.047630	5.548899	2.363743
40.H	17.095317	4.211536	2.870666
41.H	16.580021	5.432468	4.048499
42.C	10.298702	7.636690	6.413587
43.C	10.217965	8.300375	5.143750
44.C	9.422943	7.486952	4.269471
45.C	9.015190	6.325832	4.997392
46.C	9.558570	6.418142	6.324532
47.C	10.959601	8.169010	7.648618
48.H	11.768326	8.868666	7.407035
49.H	11.389252	7.361076	8.252760
50.H	10.228493	8.706431	8.272704
51.C	10.762361	9.662316	4.827358
52.H	11.682372	9.871937	5.385383
53.H	10.028105	10.438793	5.093559
54.H	10.986998	9.770978	3.760024
55.C	8.999241	7.841489	2.876694
56.H	8.873334	6.945600	2.257500

57.H	9.733672	8.486986	2.380638
58.H	8.038554	8.380232	2.893969
59.C	8.031982	5.299853	4.524953
60.H	8.190194	4.333514	5.016980
61.H	8.103977	5.140142	3.442836
62.H	7.006478	5.633690	4.752877
63.C	9.246200	5.494535	7.461142
64.H	9.141381	4.457916	7.120013
65.H	8.298758	5.794028	7.938381
66.H	10.031048	5.515589	8.225898

8

1.B	0.388513	-1.830125	0.022532
2.B	-1.285740	-1.237462	0.018933
3.B	-1.714868	0.444768	0.003133
4.B	-0.518853	1.701127	-0.020934
5.B	1.230324	1.399741	-0.023912
6.H	0.553141	-3.026487	0.033870
7.H	-2.171719	-2.060900	0.036614
8.H	-2.882693	0.748771	0.011639
9.H	-0.887006	2.853353	-0.034848
10.H	1.957927	2.363428	-0.037332
11.H	1.096806	-1.431260	-1.018419
12.H	1.100204	-1.408752	1.052742
13.H	1.642321	0.683008	-1.055307
14.H	1.656443	0.707114	1.016187
15.Mo	-0.055897	-0.011446	-1.409676
16.Mo	-0.042663	0.027351	1.407422
17.C	-1.284293	-0.865635	-3.274660
18.C	0.113866	-0.968155	-3.576469
19.C	0.658833	0.363719	-3.634118
20.C	-0.405105	1.292466	-3.367817
21.C	-1.599185	0.529243	-3.130368
22.C	-2.276767	-1.991340	-3.268351

23.H	-3.082020	-1.810321	-2.547901
24.H	-1.805873	-2.942070	-2.993578
25.H	-2.729639	-2.115896	-4.265794
26.C	0.863638	-2.239591	-3.861774
27.H	0.782080	-2.514097	-4.925513
28.H	0.476378	-3.076013	-3.268607
29.H	1.929899	-2.139913	-3.627389
30.C	2.073727	0.723563	-3.997406
31.H	2.781992	-0.051781	-3.683093
32.H	2.384365	1.660584	-3.521660
33.H	2.180824	0.849300	-5.086595
34.C	-0.323033	2.788796	-3.467252
35.H	-1.015721	3.273740	-2.770102
36.H	-0.569078	3.127305	-4.487286
37.H	0.683035	3.154392	-3.229979
38.C	-2.977710	1.093258	-2.971860
39.H	-3.455911	1.229961	-3.954780
40.H	-2.954780	2.063375	-2.465826
41.H	-3.611527	0.432146	-2.372946
42.C	-1.670473	0.064307	3.145074
43.C	-0.928134	1.291469	3.239519
44.C	0.433641	0.959789	3.538201
45.C	0.532780	-0.473861	3.638635
46.C	-0.774460	-1.027299	3.402851
47.C	-3.158076	-0.039128	2.998967
48.H	-3.650068	0.028242	3.982348
49.H	-3.446974	-0.988856	2.537390
50.H	-3.551414	0.761175	2.364541
51.C	-1.515229	2.671200	3.188251
52.H	-2.349218	2.723150	2.479810
53.H	-0.773985	3.412088	2.868788
54.H	-1.889015	2.971821	4.180800
55.C	1.547833	1.939890	3.776355
56.H	1.557285	2.278060	4.824728
57.H	1.446568	2.824708	3.136949
58.H	2.526959	1.495001	3.563626
59.C	1.765635	-1.249646	4.015355

60.H	1.849426	-1.350064	5.109295
61.H	2.678036	-0.758842	3.657363
62.H	1.750452	-2.258950	3.589162
63.C	-1.156787	-2.474085	3.531512
64.H	-0.323192	-3.136160	3.268669
65.H	-1.992034	-2.726484	2.868565
66.H	-1.456119	-2.710501	4.565735

9

1.B	-0.905984	-1.602392	0.000000
2.B	0.838132	-1.515062	0.000000
3.B	1.694402	-0.022144	0.000000
4.B	0.875059	1.491720	0.000000
5.B	-0.866359	1.623163	0.000000
6.H	-1.408408	-2.696458	0.000000
7.H	1.473158	-2.537681	0.000000
8.H	2.895074	-0.034862	0.000000
9.H	1.534421	2.498688	0.000000
10.H	-1.338778	2.730599	0.000000
11.H	-1.498645	-1.013837	-1.048729
12.H	-1.498645	-1.013837	1.048729
13.H	-1.473885	1.049919	-1.048125
14.H	-1.473885	1.049919	1.048125
15.W	-0.004879	0.000052	-1.417621
16.W	-0.004879	0.000052	1.417621
17.C	-0.663961	0.000567	-3.660470
18.C	0.160607	-1.162478	-3.453749
19.C	1.484034	-0.714881	-3.127239
20.C	1.481236	0.724972	-3.127182
21.C	0.156125	1.166615	-3.453159
22.C	-2.078823	-0.001273	-4.167662
23.H	-2.088983	0.000551	-5.269078
24.H	-2.633288	0.882688	-3.831093
25.H	-2.630154	-0.888136	-3.833784

26.C	-0.251449	-2.588804	-3.673310
27.H	0.290978	-3.268046	-3.005509
28.H	-0.042000	-2.894372	-4.710539
29.H	-1.323383	-2.733950	-3.494654
30.C	2.694112	-1.587297	-2.981413
31.H	3.427465	-1.142999	-2.298536
32.H	3.179887	-1.727432	-3.960640
33.H	2.431599	-2.575584	-2.587033
34.C	2.687353	1.602418	-2.977876
35.H	3.418388	1.163157	-2.289259
36.H	2.419184	2.591074	-2.588247
37.H	3.178285	1.741425	-3.954682
38.C	-0.262313	2.591917	-3.667865
39.H	0.274513	3.271103	-2.995383
40.H	-1.335541	2.731218	-3.492410
41.H	-0.050621	2.903136	-4.702897
42.C	-0.663961	0.000567	3.660470
43.C	0.156125	1.166615	3.453159
44.C	1.481236	0.724972	3.127182
45.C	1.484034	-0.714881	3.127239
46.C	0.160607	-1.162478	3.453749
47.C	-2.078823	-0.001273	4.167662
48.H	-2.088983	0.000551	5.269078
49.H	-2.630154	-0.888136	3.833784
50.H	-2.633288	0.882688	3.831093
51.C	-0.262313	2.591917	3.667865
52.H	0.274513	3.271103	2.995383
53.H	-0.050621	2.903136	4.702897
54.H	-1.335541	2.731218	3.492410
55.C	2.687353	1.602418	2.977876
56.H	3.418388	1.163157	2.289259
57.H	3.178285	1.741425	3.954682
58.H	2.419184	2.591074	2.588247
59.C	2.694112	-1.587297	2.981413
60.H	3.427465	-1.142999	2.298536
61.H	2.431599	-2.575584	2.587033
62.H	3.179887	-1.727432	3.960640

63.C	-0.251449	-2.588804	3.673310
64.H	0.290978	-3.268046	3.005509
65.H	-1.323383	-2.733950	3.494654
66.H	-0.042000	-2.894372	4.710539

10

Cr	-4.414531	6.648116	12.765906
Cr	-6.092263	4.730283	12.760217
B	-5.222909	5.656698	14.531531
B	-4.103143	4.682579	13.632537
B	-4.060330	4.649658	11.996977
B	-5.128664	5.587817	11.002218
H	-5.232463	5.661415	15.738868
H	-3.367198	4.015093	14.315569
H	-3.293969	3.955481	11.376771
H	-5.059480	5.563376	9.796921
H	-6.376713	5.328012	11.209405
H	-5.106736	6.859076	11.252321
H	-5.144156	6.918433	14.257483
H	-6.462383	5.425833	14.247386
C	-2.357108	7.204562	13.386037
C	-3.283811	8.143955	13.939178
C	-3.979921	8.791006	12.855746
C	-3.427622	8.282323	11.633685
C	-2.446890	7.287725	11.956112
C	-6.891040	3.021330	13.933273
C	-7.991670	3.836143	13.481016
C	-7.990790	3.826718	12.058197
C	-6.890870	3.000736	11.620835
C	-6.215381	2.507276	12.781277
C	-9.021773	4.489878	14.355632
C	-9.021657	4.465077	11.173683
C	-6.574297	2.624926	10.206016
C	-5.109292	1.496403	12.792301

C	-6.574499	2.671466	15.354953
C	-3.416829	8.480680	15.394518
C	-4.964377	9.917249	12.984204
C	-3.742412	8.785729	10.255711
C	-1.556478	6.576055	10.983666
C	-1.347589	6.403310	14.150682
H	-9.865477	3.804214	14.534184
H	-9.426597	5.399356	13.894601
H	-8.609277	4.766499	15.333519
H	-9.862813	3.774319	11.002008
H	-8.608815	4.731489	10.193104
H	-9.430600	5.378682	11.622679
H	-5.491108	2.543043	10.049678
H	-6.955943	3.365571	9.493041
H	-7.027686	1.652616	9.954374
H	-5.528319	0.476815	12.810446
H	-4.466487	1.615551	13.672266
H	-4.474070	1.587069	11.903606
H	-6.955300	3.425763	16.053846
H	-5.491312	2.592349	15.512689
H	-7.028466	1.704306	15.625109
H	-3.281637	7.595646	16.028197
H	-4.400218	8.908571	15.625811
H	-2.654683	9.221672	15.683481
H	-4.449384	10.891746	13.024060
H	-5.566209	9.826424	13.896858
H	-5.658218	9.945866	12.135144
H	-4.762870	9.183626	10.190736
H	-3.641902	7.995680	9.501942
H	-3.050990	9.599039	9.984574
H	-0.614561	7.132320	10.847431
H	-2.031260	6.473420	10.000714
H	-1.307465	5.567701	11.335666
H	-1.694602	6.178686	15.166021
H	-0.400449	6.961798	14.232710
H	-1.137409	5.448090	13.655288

11

1.Cr	-6.328604	4.797600	12.669710
2.Cr	-4.526694	6.890786	12.786073
3.B	-5.756602	6.015942	14.371263
4.B	-4.523174	4.981982	13.820237
5.B	-4.208351	4.848276	12.204256
6.B	-5.142109	5.711009	11.073151
7.H	-6.182448	6.076604	15.493923
8.H	-3.929137	4.414937	14.700487
9.H	-3.362171	4.150465	11.708160
10.H	-4.908472	5.817876	9.898674
11.H	-6.424725	5.396593	11.097708
12.H	-5.565554	7.283501	14.052776
13.C	-6.072121	2.573925	12.459749
14.C	-6.554919	2.864073	13.781191
15.C	-7.827979	3.501916	13.657400
16.C	-8.134620	3.621437	12.251745
17.C	-7.046279	3.044687	11.520543
18.C	-3.692179	8.917483	12.907732
19.C	-3.273035	8.188511	14.067244
20.C	-2.458718	7.090207	13.638682
21.C	-2.376422	7.133244	12.205142
22.C	-3.129084	8.260732	11.751958
23.C	-1.664937	6.186207	14.530509
24.C	-3.545440	8.562644	15.493893
25.C	-4.435265	10.220236	12.909767
26.C	-3.174865	8.762626	10.339793
27.C	-1.479843	6.289007	11.351601
28.C	-5.946147	2.383102	15.063056
29.C	-8.751423	3.823485	14.794188
30.C	-9.429183	4.102705	11.666962
31.C	-6.975844	2.863243	10.033352
32.C	-4.871344	1.740253	12.134161
33.H	-9.331009	2.928584	15.071421

34.H	-9.464113	4.614424	14.534024
35.C	-7.493266	6.143654	13.147593
36.C	-5.773798	7.648129	11.659714
37.H	-8.196659	4.150386	15.682082
38.H	-10.145202	3.269554	11.587271
39.H	-9.287719	4.516581	10.661438
40.H	-9.891243	4.882619	12.283006
41.H	-5.949495	2.975430	9.663046
42.H	-7.602110	3.592009	9.505717
43.H	-7.327054	1.857167	9.755186
44.H	-5.135399	0.671056	12.186267
45.H	-4.050639	1.923098	12.837199
46.H	-4.496346	1.945619	11.125248
47.H	-6.135579	3.079458	15.888614
48.H	-4.861524	2.258847	14.973754
49.H	-6.379429	1.407103	15.337596
50.H	-3.672014	7.674439	16.124868
51.H	-4.453282	9.169940	15.587213
52.H	-2.707156	9.149460	15.901014
53.H	-3.728840	11.062180	12.981179
54.H	-5.123335	10.290195	13.760657
55.H	-5.025447	10.355637	11.996241
56.H	-4.068216	9.367758	10.147163
57.H	-3.168665	7.935328	9.619677
58.H	-2.293951	9.391817	10.135690
59.H	-0.507139	6.792039	11.223067
60.H	-1.906803	6.122667	10.355455
61.H	-1.296785	5.308255	11.803705
62.H	-2.137648	6.067260	15.511914
63.H	-0.658562	6.608046	14.687947
64.H	-1.551046	5.187515	14.093631
65.O	-6.486287	8.272828	10.962801
66.O	-8.355888	6.894873	13.420908

12

1.Cr	-6.289813	4.774628	12.738848
2.Cr	-4.480578	6.826442	12.749237
3.B	-5.290013	5.727159	11.031228
4.B	-4.250953	4.806091	12.013302
5.B	-4.329349	4.867226	13.649218
6.B	-5.459566	5.850681	14.456068
7.H	-5.524952	5.899522	15.661000
8.H	-3.628132	4.214089	14.382637
9.H	-3.479278	4.108422	11.402650
10.H	-5.231047	5.698665	9.825287
11.H	-6.580235	5.504452	11.269097
12.H	-5.263931	7.034499	11.299155
13.H	-5.374299	7.137140	14.117431
14.H	-6.724650	5.638286	14.090788
15.H	-9.728093	3.250946	14.710569
16.H	-9.571523	4.905161	14.084935
17.C	-2.392100	7.093601	13.463483
18.C	-3.196327	8.179025	13.938091
19.C	-3.711132	8.887249	12.802696
20.C	-3.212423	8.241322	11.623681
21.C	-2.402140	7.131759	12.027924
22.C	-6.728849	2.929109	13.904957
23.C	-7.953581	3.582328	13.546444
24.C	-8.043269	3.603705	12.117025
25.C	-6.875081	2.957955	11.592923
26.C	-6.065180	2.539776	12.695955
27.C	-9.010217	4.058790	14.498120
28.C	-9.211780	4.091996	11.313902
29.C	-6.599660	2.665061	10.149027
30.C	-4.848140	1.670830	12.611060
31.C	-6.290746	2.576719	15.294113
32.C	-3.370198	8.569309	15.375637
33.C	-4.480432	10.174868	12.844385
34.C	-3.406980	8.713515	10.213388
35.C	-1.550115	6.295996	11.122424
36.C	-1.524652	6.212194	14.308709
37.H	-7.390486	5.910586	12.631897

38.H	-5.740176	7.775144	12.661255
39.H	-8.578321	4.379048	15.453649
40.H	-9.925626	3.272179	11.136278
41.H	-8.897729	4.476124	10.336140
42.H	-9.746132	4.897422	11.830651
43.H	-5.526615	2.718333	9.928421
44.H	-7.110942	3.373596	9.486613
45.H	-6.950191	1.652897	9.891216
46.H	-5.145358	0.610194	12.663541
47.H	-4.152403	1.872301	13.433665
48.H	-4.306415	1.825753	11.671364
49.H	-6.698123	3.273318	16.036423
50.H	-5.198194	2.595472	15.384667
51.H	-6.638446	1.564508	15.557162
52.H	-3.427033	7.688573	16.026800
53.H	-4.282996	9.157324	15.528937
54.H	-2.518049	9.181563	15.710613
55.H	-3.790459	11.032630	12.882739
56.H	-5.129848	10.228717	13.725764
57.H	-5.114918	10.294343	11.958800
58.H	-4.341390	9.276076	10.099556
59.H	-3.433324	7.874153	9.508143
60.H	-2.579633	9.376787	9.915292
61.H	-0.570899	6.781208	10.975429
62.H	-2.012976	6.164603	10.137279
63.H	-1.376404	5.298481	11.541065
64.H	-1.957767	6.050033	15.302469
65.H	-0.534181	6.678491	14.441449
66.H	-1.379729	5.228887	13.847284

13

1.B	-0.302045	7.215541	10.505028
2.B	-1.668027	6.204304	10.352312
3.B	1.369755	6.786852	10.511129

4.B	0.607724	7.599980	11.920753
5.H	0.071912	4.694605	12.172734
6.H	-0.753828	8.066766	9.776903
7.H	1.588372	5.541316	10.792599
8.H	2.159421	7.214838	9.713124
9.H	1.867569	7.227166	11.667299
10.H	0.756890	8.723202	12.317894
11.H	0.457101	6.748705	12.889489
12.H	-2.680053	6.370236	9.731984
13.Cr	-0.971701	6.043682	12.241424
14.Cr	-0.032743	5.033149	10.501817
15.C	-2.910350	7.024323	12.926170
16.C	-1.881632	7.325474	13.861788
17.C	-1.391513	6.081770	14.411387
18.C	-2.149974	5.022341	13.820149
19.C	-3.072883	5.596246	12.891477
20.C	0.910326	3.110411	9.971854
21.C	-0.523767	2.992648	9.963282
22.C	-1.033577	3.843085	8.924280
23.C	0.090222	4.457882	8.270632
24.C	1.274974	3.990452	8.898085
25.C	0.015024	5.365319	7.080019
26.C	-2.443966	3.852059	8.414705
27.C	-1.318606	2.007686	10.768400
28.C	1.855879	2.307981	10.818709
29.C	2.674673	4.326654	8.481599
30.C	-1.464887	8.696723	14.299537
31.C	-0.409954	5.936836	15.537804
32.C	-2.058638	3.574392	14.202436
33.C	-4.154758	4.865115	12.153925
34.C	-3.769161	8.019257	12.206334
35.H	-0.895148	5.977052	7.100754
36.H	0.005700	4.782098	6.144938
37.H	0.872033	6.048235	7.037517
38.H	-2.580361	3.049262	7.671626
39.H	-2.696100	4.802922	7.931912
40.H	-3.170042	3.688377	9.219782

41.H	-1.344300	1.028998	10.261279
42.H	-2.356280	2.335702	10.899750
43.H	-0.885770	1.850481	11.763419
44.H	2.792724	2.847502	11.005059
45.H	2.115195	1.355038	10.329162
46.H	1.416171	2.068105	11.794328
47.H	2.999968	3.654211	7.672306
48.H	3.384454	4.214525	9.309960
49.H	2.753246	5.355879	8.111986
50.H	-0.415899	8.722821	14.617080
51.H	-2.079910	9.030908	15.150274
52.H	-1.580298	9.430943	13.493796
53.H	-0.923528	5.957319	16.512886
54.H	0.329086	6.747333	15.538391
55.H	0.139442	4.989260	15.475188
56.H	-2.403702	2.917074	13.396965
57.H	-2.685727	3.373783	15.086001
58.H	-1.031541	3.284098	14.455596
59.H	-5.091291	4.881776	12.734742
60.H	-3.892248	3.813584	11.986530
61.H	-4.360019	5.321178	11.178123
62.H	-4.640791	8.292103	12.823284
63.H	-4.143166	7.616129	11.257816
64.H	-3.217914	8.940136	11.981113

14

1.Cr	0.574707	0.888768	0.733932
2.Cr	-0.800903	-0.113375	-0.984676
3.B	-1.614670	1.273460	0.550208
4.B	-1.071133	-0.276190	1.021473
5.B	1.227332	-0.201170	-0.856168
6.B	0.811143	1.351417	-1.434110
7.H	-1.864816	1.371377	-0.694134
8.H	-2.597378	1.539440	1.196886

9.H	-1.482629	-1.056336	1.834891
10.H	-0.722466	2.173729	0.725335
11.H	-0.362646	1.418139	-1.922136
12.H	2.122430	-0.944530	-1.145643
13.H	1.624990	1.679876	-2.261374
14.H	0.771206	2.221664	-0.497105
15.C	-0.586796	-2.092239	-1.897092
16.C	-0.855536	-1.151260	-2.949880
17.C	-2.148078	-0.588358	-2.718283
18.C	-2.681489	-1.154987	-1.519246
19.C	-1.721070	-2.096553	-1.008027
20.C	0.827858	0.687641	2.941311
21.C	1.704050	-0.233193	2.276676
22.C	2.627462	0.512272	1.467962
23.C	2.301035	1.901552	1.614409
24.C	1.193132	2.006793	2.526009
25.C	-0.157328	0.355106	4.020605
26.C	1.729307	-1.718316	2.481004
27.C	3.864881	-0.023527	0.813025
28.C	3.078099	3.038599	1.019978
29.C	0.591998	3.279465	3.046558
30.C	0.025143	-0.891116	-4.133564
31.C	-2.842213	0.407920	-3.601231
32.C	-4.042809	-0.902104	-0.947066
33.C	-1.978309	-3.122119	0.055843
34.C	0.519618	-3.104767	-1.884033
35.H	-0.512925	-0.677706	3.939996
36.H	0.314436	0.474628	5.009487
37.H	-1.035303	1.011398	3.985685
38.H	2.105132	-2.238328	1.591716
39.H	2.389960	-1.977079	3.324224
40.H	0.730162	-2.109871	2.705339
41.H	4.105538	0.518010	-0.109708
42.H	4.721841	0.076276	1.499134
43.H	3.762183	-1.083233	0.555487
44.H	2.468803	3.946520	0.936376
45.H	3.951598	3.280868	1.646118

46.H	3.445015	2.791391	0.016258
47.H	-0.474058	3.158473	3.272986
48.H	1.097051	3.592170	3.974287
49.H	0.688714	4.099836	2.325403
50.H	-0.097330	0.130511	-4.513469
51.H	1.083126	-1.023114	-3.878456
52.H	-0.215925	-1.583945	-4.955717
53.H	-3.521977	1.052642	-3.031987
54.H	-2.128697	1.051634	-4.128719
55.H	-3.442417	-0.114693	-4.362854
56.H	-4.044394	-1.022539	0.142732
57.H	-4.392725	0.114011	-1.166469
58.H	-4.778380	-1.606138	-1.368073
59.H	-1.060660	-3.391625	0.592218
60.H	-2.703153	-2.769287	0.797437
61.H	-2.381315	-4.040215	-0.402850
62.H	1.407916	-2.747144	-2.415445
63.H	0.824657	-3.360344	-0.862170
64.H	0.180925	-4.032215	-2.374609

15

1.B	0.094200	-1.292325	-0.011716
2.B	-1.156421	-0.062656	-0.013095
3.B	-0.102996	1.337113	-0.018302
4.H	-0.119800	-2.482859	-0.009343
5.H	-2.360038	-0.148832	-0.012478
6.H	-0.484803	2.484728	-0.021038
7.H	0.995168	-1.010066	-0.932215
8.H	0.831841	1.185302	-0.938071
9.H	0.996606	-1.006774	0.906019
10.H	0.833558	1.189478	0.900153
11.Co	-0.037645	0.016795	-1.695728
12.Co	-0.034155	0.025557	1.666625
13.C	-0.037237	-1.166572	-3.378055

14.C	0.735847	0.019934	-3.630139
15.C	-0.120606	1.152782	-3.409427
16.C	-1.427593	0.670506	-3.032010
17.C	-1.375920	-0.770929	-3.014957
18.C	-0.057426	1.155709	3.386790
19.C	0.748884	-0.014514	3.596095
20.C	-0.077462	-1.165018	3.341849
21.C	-1.399480	-0.708767	2.990497
22.C	-1.386569	0.733433	3.012754
23.C	2.181145	-0.033976	4.039409
24.C	0.341458	-2.598556	3.454021
25.C	-2.593616	-1.577728	2.745564
26.C	-2.563443	1.630040	2.784290
27.C	0.382421	2.577716	3.555018
28.C	2.164732	0.065747	-4.082399
29.C	0.255292	2.593645	-3.571137
30.C	-2.642327	1.513259	-2.796807
31.C	-2.527374	-1.693524	-2.762103
32.C	0.443171	-2.579929	-3.500076
33.H	2.251623	-0.051064	5.139039
34.H	2.724216	0.851577	3.687771
35.H	2.708747	-0.917840	3.661228
36.H	-0.123247	-3.211993	2.672066
37.H	0.043553	-3.013774	4.429925
38.H	1.428570	-2.709701	3.362808
39.H	-3.281965	-1.115994	2.028015
40.H	-3.144103	-1.748850	3.685077
41.H	-2.302174	-2.555734	2.344356
42.H	-2.253263	2.606261	2.392747
43.H	-3.108035	1.802158	3.727052
44.H	-3.263525	1.190458	2.063948
45.H	-0.084192	3.230818	2.807001
46.H	1.469860	2.678911	3.455798
47.H	0.101221	2.954499	4.551327
48.H	2.228908	0.052457	-5.182493
49.H	2.734342	-0.793515	-3.708361
50.H	2.669433	0.974810	-3.733552

51.H	-0.229382	3.219834	-2.811612
52.H	-0.054327	2.965916	-4.560655
53.H	1.338481	2.740893	-3.484150
54.H	-2.373952	2.503608	-2.409913
55.H	-3.316845	1.044342	-2.070657
56.H	-3.200289	1.657884	-3.736365
57.H	-3.233850	-1.260693	-2.044131
58.H	-2.188932	-2.654788	-2.357240
59.H	-3.072793	-1.894994	-3.698525
60.H	0.011886	-3.216390	-2.717275
61.H	1.534850	-2.643799	-3.418457
62.H	0.155399	-3.003865	-4.475279

16

1.Rh	5.209461	1.388461	5.406134
2.Rh	6.427074	2.934151	3.499208
3.B	4.777555	3.557494	4.636059
4.B	6.384042	4.321636	5.050832
5.B	7.134748	2.704524	5.457996
6.H	3.794086	4.108086	4.195191
7.H	6.830096	5.429754	4.914556
8.H	8.285146	2.485039	5.762847
9.H	4.327158	2.807497	5.665267
10.H	5.182606	4.470782	5.576817
11.H	6.899393	3.857455	6.170081
12.H	6.396246	2.071183	6.398319
13.C	3.973516	-0.240946	4.516024
14.C	3.417625	0.139771	5.798838
15.C	4.380534	-0.141326	6.822504
16.C	5.559305	-0.658417	6.164395
17.C	5.295260	-0.759727	4.751773
18.C	3.216507	-0.280011	3.223119
19.H	2.629079	-1.209668	3.142685
20.H	3.892268	-0.236032	2.362411

21.H	2.517308	0.560998	3.139641
22.C	2.026844	0.658669	6.016095
23.H	1.313339	-0.175415	6.109200
24.H	1.697545	1.285982	5.179040
25.H	1.958586	1.259150	6.931044
26.C	4.177178	-0.010013	8.304594
27.H	3.773388	-0.942652	8.731579
28.H	3.472534	0.795484	8.546533
29.H	5.118406	0.208998	8.824204
30.C	6.802185	-1.139294	6.853634
31.H	6.714812	-2.207025	7.110561
32.H	6.985609	-0.587818	7.783525
33.H	7.686332	-1.019731	6.216191
34.C	6.170442	-1.461461	3.760954
35.H	5.990704	-2.548986	3.792112
36.H	7.233747	-1.295493	3.969627
37.H	5.970896	-1.122719	2.739129
38.C	8.172879	3.435299	2.173306
39.C	7.051678	4.285946	1.827634
40.C	6.018289	3.455558	1.268831
41.C	6.485012	2.107228	1.290029
42.C	7.815506	2.086280	1.852106
43.C	9.515128	3.905351	2.653826
44.H	10.183649	4.125436	1.805208
45.H	10.006996	3.148592	3.277151
46.H	9.429892	4.819895	3.253200
47.C	7.045765	5.786744	1.853601
48.H	7.431040	6.192084	0.903550
49.H	7.673055	6.181854	2.661829
50.H	6.033502	6.184779	1.997598
51.C	4.733083	3.941051	0.664096
52.H	4.865144	4.198117	-0.400144
53.H	4.361068	4.837463	1.175504
54.H	3.944460	3.180425	0.723331
55.C	5.802820	0.954908	0.617967
56.H	6.072630	0.918539	-0.450809
57.H	4.710335	1.037352	0.671395

58.H	6.095383	-0.009009	1.050952
59.C	8.734774	0.900451	1.900314
60.H	9.323382	0.812286	0.971566
61.H	8.181610	-0.038368	2.024646
62.H	9.445722	0.976575	2.732636

16b

1.Rh	6.766429	3.489795	8.729300
2.Rh	6.007495	3.281949	6.100244
3.B	6.660843	5.105549	6.992101
4.B	7.878087	4.258407	5.933105
5.B	7.831587	2.817520	7.054303
6.H	6.065415	6.136070	6.791261
7.H	8.320567	4.464479	4.833884
8.H	8.488220	1.800745	6.983721
9.H	7.034645	5.129517	8.252250
10.H	7.907600	5.423970	6.556101
11.H	8.810747	3.738215	6.672825
12.H	5.383770	3.314550	7.738685
13.C	5.012144	1.467954	5.084883
14.C	5.804607	2.201314	4.147206
15.C	5.231248	3.535515	4.022674
16.C	4.072748	3.604613	4.868009
17.C	3.965278	2.348722	5.548407
18.C	6.535958	1.766922	10.086426
19.C	5.578879	2.737657	10.617382
20.C	6.290187	3.886435	10.998669
21.C	7.715050	3.648489	10.737987
22.C	7.863506	2.308122	10.255979
23.C	4.104727	2.502747	10.755408
24.C	5.733553	5.134107	11.618933
25.C	8.823734	4.573931	11.151549
26.C	9.148129	1.561797	10.059151
27.C	6.214962	0.350160	9.710222

28.C	6.933382	1.656326	3.322031
29.C	5.658120	4.583825	3.037150
30.C	3.109571	4.752040	4.958253
31.C	2.856591	1.954877	6.479451
32.C	5.160756	0.015766	5.433512
33.H	3.879823	1.949221	11.681627
34.H	3.709523	1.913250	9.918948
35.H	3.545441	3.445502	10.790714
36.H	5.855790	5.119474	12.714309
37.H	4.663361	5.249677	11.408151
38.H	6.242582	6.032971	11.247604
39.H	9.055765	4.449771	12.222411
40.H	8.553747	5.626146	10.995122
41.H	9.743960	4.379630	10.587477
42.H	9.400451	0.979078	10.959980
43.H	9.983157	2.243422	9.858120
44.H	9.083958	0.865829	9.214561
45.H	6.230411	-0.305809	10.596336
46.H	6.940376	-0.045045	8.989066
47.H	5.218376	0.269713	9.258460
48.H	6.559912	1.242380	2.371452
49.H	7.465079	0.855042	3.849173
50.H	7.666517	2.435130	3.079650
51.H	5.147220	4.440560	2.071227
52.H	6.738223	4.547965	2.851000
53.H	5.416583	5.592532	3.394361
54.H	2.321405	4.672255	4.191517
55.H	3.615057	5.714730	4.812761
56.H	2.613913	4.787980	5.936301
57.H	2.017456	1.514320	5.917431
58.H	2.466658	2.816830	7.033766
59.H	3.189373	1.207235	7.209517
60.H	4.560896	-0.620554	4.761933
61.H	4.831110	-0.190342	6.459564
62.H	6.204707	-0.311309	5.352962

17

1.Ir	5.227488	1.427010	5.457160
2.Ir	6.452436	2.943578	3.484679
3.B	4.847267	3.569454	4.678039
4.B	6.503127	4.324071	5.054878
5.B	7.190808	2.631938	5.412610
6.H	3.828568	4.118602	4.345588
7.H	6.965459	5.429760	4.961823
8.H	8.301642	2.327257	5.763442
9.H	4.424500	2.844391	5.834455
10.H	5.312418	4.474587	5.613555
11.H	7.030753	3.803604	6.144178
12.H	6.383977	2.092421	6.464544
13.C	3.957113	-0.170537	4.539389
14.C	3.419408	0.179034	5.834589
15.C	4.403378	-0.124788	6.843416
16.C	5.567397	-0.656905	6.163029
17.C	5.290675	-0.705943	4.752012
18.C	3.187566	-0.184243	3.254644
19.H	2.615333	-1.121192	3.154411
20.H	3.854642	-0.105129	2.390549
21.H	2.475665	0.648074	3.202285
22.C	2.025337	0.670616	6.088615
23.H	1.334085	-0.181180	6.189040
24.H	1.663624	1.297665	5.264965
25.H	1.965434	1.259734	7.011367
26.C	4.206698	-0.048135	8.328401
27.H	3.785407	-0.990612	8.714258
28.H	3.518887	0.760234	8.603567
29.H	5.153526	0.130089	8.852014
30.C	6.800347	-1.196294	6.825581
31.H	6.681444	-2.270168	7.040633
32.H	7.005628	-0.687324	7.774831
33.H	7.683342	-1.079053	6.186235
34.C	6.150002	-1.388858	3.735428
35.H	5.955233	-2.473948	3.741149

36.H	7.216215	-1.239478	3.939742
37.H	5.945089	-1.019468	2.726417
38.C	8.127315	3.413690	2.098916
39.C	6.988159	4.252907	1.769053
40.C	5.943122	3.401688	1.256327
41.C	6.422394	2.054045	1.281015
42.C	7.767168	2.048330	1.809851
43.C	9.492202	3.898288	2.491590
44.H	10.111946	4.084371	1.599036
45.H	10.016118	3.162050	3.113469
46.H	9.439504	4.834291	3.060535
47.C	6.977910	5.752879	1.761089
48.H	7.349208	6.136557	0.796984
49.H	7.614642	6.165061	2.552917
50.H	5.966242	6.149827	1.910696
51.C	4.635645	3.862494	0.682614
52.H	4.731740	4.080656	-0.394020
53.H	4.279680	4.775827	1.174447
54.H	3.853174	3.101980	0.796834
55.C	5.738819	0.899633	0.613654
56.H	5.983602	0.890323	-0.461585
57.H	4.646958	0.963431	0.692890
58.H	6.058591	-0.067570	1.017661
59.C	8.704113	0.875625	1.831510
60.H	9.280732	0.811236	0.893384
61.H	8.166196	-0.072581	1.949090
62.H	9.424223	0.950609	2.655709